Flood Forecasting in the Sparsely Gauged Jhelum River Basin of Greater Himalayas Using Integrated Hydrological and Hydraulic Modelling Approach

Sabah Parvaze (sabah.allaie@gmail.com)
Sher-E-Kashmir University of Agricultural Sciences and Technology Kashmir
Junaid Nazir Khan
Sher-E-Kashmir University of Agricultural Sciences and Technology Kashmir
Rohitashw Kumar
Sher-E-Kashmir University of Agricultural Sciences and Technology Kashmir
Saqib Parvaze Allaie
Sam Higginbottom University of Agriculture Technology and Sciences

Research Article

Keywords: ECMWF, Error updating, Flood Forecast, Jhelum, Lead Time, MIKE 11 Snowmelt

Posted Date: May 6th, 2021

DOI: https://doi.org/10.21203/rs.3.rs-461873/v1

Flood Forecasting in the Sparsely Gauged Jhelum River Basin of Greater Himalayas Using Integrated Hydrological and Hydraulic Modelling Approach

Sabah Parvaze[1*], Junaid Nazir Khan[1], Rohitashw Kumar[1], and Saqib Parvaze Allaie[2]

[1] Sher-e-Kashmir University of Agricultural Sciences and Technology of Kashmir, Shalimar, Srinagar, Jammu and Kashmir, 190025

[2] Sam Higginbottom University of Agriculture, Technology and Sciences, Allahabad, Uttar Pradesh, 211007

Abstract

Flood forecasting using hydrological and hydraulic models is an efficient non-structural flood management option. For real-time flood forecasting in the data scarce Jhelum basin, the present study evaluated the capability of MIKE 11 Nedbor-Afstromings Model (NAM), hydrodynamic (HD) and flood forecasting (FF) models to forecast streamflow of four principal gauging stations of river Jhelum (Sangam, Ram Munshi Bagh, Asham and Baramulla). European Centre for Medium-Range Weather Forecast (ECMWF) model-forecasted precipitation and temperature data was used to increase the forecast lead time to 7 days. The forecast results were assessed by calculating coefficient of determination (R^2), Nash-Sutcliffe Efficiency (NSE) and various error indices. Integration of the MIKE 11 NAM and HD modules improved the results of MIKE 11 NAM significantly. Values of R^2 improved by 8-15% while that of NSE improved by 8-14% at various stations by using integrated model. MIKE 11 FF with ECMWF input was used to simulate the streamflow with lead times of 1to 10-days. The forecast results were efficient for lead times up to 7-days with R^2 and NSE values 0.8 and 0.7, respectively. Peak error for 7-days forecast was 19.1% and the peak time error was 1.2 h. The developed model can be used for short to medium range flood forecasting for the data scarce, snow dominated Jhelum basin and can apply to similar basins around the globe as a component of the early flood warning system.

Keywords: ECMWF, Error updating, Flood Forecast, Jhelum, Lead Time, MIKE 11 Snowmelt.

1. Introduction

Floods, along with debris flow, are a significant threat to people living in mountainous regions. The frequency of devastating flood disasters in the high mountain areas of the world has increased tremendously during the past few decades (Kumar et al. 2018). The Himalayan

region, without exception to the global trend, witnessed some calamitous hydrological catastrophes in the recent past. Floods are recognized as the foremost physical hazard for sustainable development in the Himalayas. The most recent floods in the Himalayas include the Kosi floods of 2008, the Leh flash floods and Ganga floods of 2010, Brahmaputra floods of 2012, Kedarnath flash floods of 2013, and the Jhelum floods of 2014. Kashmir Valley, in the Greater Himalayas, is one of the most susceptible flood hazard-prone regions in the Himalayas (Sen 2010; Altaf et al. 2013). Throughout its history, Kashmir valley was inundated by many floods, causing an enormous loss of life and property (Singh and Kumar 2013). Kashmir valley is characterized by a relatively flat alluvial plain surrounded by high mountain ranges (Dar et al. 2015). River Jhelum makes up the trunk-order stream, occupying the lower-most furrow of the alluvial plain. The river serves as the destination for all the water bodies, draining the Kashmir valley's length and breadth. The hydrographic features of the river Jhelum and geological setup of the Kashmir valley render it extremely vulnerable to flood hazards. About 30 major floods have been recorded in the history of Kashmir valley. Some prominent flood years of the recent past are 1963, 1994, 1996, 2004, 2006, and 2014 (Meraj et al. 2015; Kumar and Acharya 2016).

Prolonged torrential rainfalls, with sped up snowmelt, are the primary cause of floods in Kashmir valley. Their effect is exacerbated by factors such as urban expansion, wetland degradation, encroachment of waterways, landfilling, and road/railway construction in the floodplain (Ahmad et al. 2019). Another major factor leading to floods is the insufficient carrying capacity of the river Jhelum. The safe carrying capacity of the Jhelum from Sangam to Wular Lake varies from 850 to 1500 cumecs. For the Srinagar city, this value is merely about 990 cumecs. The flood that inundated the entire Kashmir Valley in September-2014 was declared as the highest ever flood recorded on the River Jhelum. The discharge was about 3263 cumecs at upstream Sangam and about 2055 cumecs downstream at Ram Munshi Bagh. Most parts of the Valley, including the capital city of Srinagar, were submerged, resulting in colossal loss of life and property (Alam et al. 2018). A flood spill channel with a carrying capacity of 480 cumecs was constructed at Padshahi Bagh in 1903 to regulate the flow of Jhelum as it passes through the Srinagar City. At present, carrying capacity has decreased to nearly 20% of the designed capacity (Bhat et al. 2019). Most settlements in Kashmir Valley are on the banks of river Jhelum, including the capital city of Srinagar. Rapid rise of flood water in the densely populated flood plain poses a substantial risk to life and property. The devastating flood of 2014 highlighted the need for flood forecasting and early warning system in the valley.

The Central Water Commission, India's leading water resources body in authority for flood forecasts and associated advisories to states, has no forecast system for any place in Kashmir Valley. Flood forecasts are synonymous to meteorological forecasts. When meteorological conditions conducive to heavy rainfall are foreseen for an area, a watch is issued on radio and television. This alerts residents of the potential occurrence of rainfall that could produce flooding. Rainfall forecasts do not always benefit the flood-vulnerable population. Although the information is mostly correct, yet it does not always benefit the inhabitants. This is because of insufficient lead time of the warnings and limited outreach of the warning. Also, floods are not merely a meteorological phenomenon. These occur when specific meteorological and hydrological conditions co-exist (Creutin et al. 2013). Floods not only depend on intensity and duration of rainfall, but also on the hydrological characteristics the basin. These characteristics include drainage area, baseflow, antecedent moisture content condition, discharge, land use, land cover, and topography of the basin (Borsch and Simonov 2016). A flood forecasting system based on the hydrologic characteristics of the basin to give early flood alerts is essential for the region.

In the present study, a deterministic approach was used to generate a flood forecasting system for Kashmir Valley. Deterministic flood forecasting models require two crucial elements: 1) mechanisms for flood generation, such as precipitation formation, snowmelt modelling, catchment runoff within hydrologic models, and 2) flood routing. Deterministic rainfall-runoff models involve elements for the different hydrological and associated processes, like precipitation, infiltration, and soil moisture dynamics, evapotranspiration, runoff production, and streamflow routing. Precipitation is a critical input to these models, and depth of flow and runoff would be the key outputs Flood routing methods may be categorized as hydraulic or hydrologic. when the time-varying flow is computed at a single specified location downstream, it is hydrologic routing. However, when the hydrograph is concurrently calculated at several cross-sections across the watercourse, it is called hydraulic flood routing.

An operational flood forecasting system may use both hydrologic and hydraulic models for real-time forecasting. Many researchers and agencies have applied these models to various river basins globally for flood simulation and mitigation. (De Roo et al. 2003) developed a flood forecasting system for European test basins. They applied real-time rainfall and rainfall forecasts from global numerical weather prediction models, grids of coarse resolution for forecasting floods at the basin scale. European Flood Alert System (EFAS) by (Thielen et al. 2009) was a physically based, distributed hydrological model LISFLOOD and gave a lead time

of 3-10 days for flood forecast. Rahman et al. 2012 developed a flood forecasting and warning system for Bangladesh using an integrated RR and hydraulic routing model of MIKE 11 software. A web-based flood forecasting system based on HEC-HMS was applied for the Philippines by (Alfredo Mahar et al. 2017). Model-based flood forecasting and warning systems have been successfully implemented to issue timely flood warnings to the end-users. Some notable applications have been for Yangtze river and Han river in China (Liu et al. 2008), Po basin in Italy (Di Baldassarre et al. 2009), Chenab basin in Pakistan (Asghar et al. 2019) and Vu Gia–Thu Bon river basin, Vietnam (Loi et al. 2019). In India, the Central Water Commission (CWC) and National Institute of Disaster Management (NIDM) have implemented model-based flood forecasting systems for Damodar Basin, Godavari Basin, Mahanadi Basin, and Chambal Basin.

This study focuses on applying an integrated hydrologic and hydraulic approach using MIKE 11, a software by Danish Hydraulic Institute (DHI) comprising rainfall-runoff (*Nedbor-Afstromings Model* or NAM), hydrodynamic (HD), and flood forecasting (FF) model to develop a flood forecasting system for the Jhelum river basin in the mountain-bound Kashmir Valley. Heavy rains, together with snowmelt from upper reaches, generate floods in low-lying areas. The rapidness of floods limits the time available for flood warnings to be prepared and issued. This provides a minimal opportunity for the people to make necessary preparations. The absence of a flood forecasting and early warning system results in much higher devastation and panic than it is supposed to be. Even after the devastating flood of September 2014, which left nearly 3.5% geographical area of the valley submerged and killing nearly 300 people, there has been no implementation of an operational flood forecasting system in the region. Although some studies for simulation and prediction of floods have been conducted using neural networks (Tabbussum and Dar 2021), statistical approaches (Parvaze et al. 2021), hydrological models (Meraj et al. 2018) and other soft computing techniques (Himayoun et al. 2020), real time flood forecasting has yet not been implemented in the basin. The key component of the study is the use of a combination of hydrological and hydraulic model, on the river basin using open-source, geospatial, meteorological and hydrological information. Rainfall-runoff simulation is modelled together with snowmelt for real-time flood prediction in a data-scarce region. Satellite-based forecasted temperature and precipitation data was used to enhance the reliability of the model and increase the time of forecast (Vallejo Orti and Negussie 2019) . For reducing the uncertainties in the flood forecasts arising from inconsistencies in input data,

model structure, parameter values and satellite data, an updating procedure was included in the flood forecasting system.

2. Study Area and Data

2.1. Study Area

Kashmir Valley is a part of the Western Himalayas and bound by the Greater Himalaya to the northeast and the Pir Panjal Range to the southwest (Fig. 1). The bowl-shaped valley has a total area of about 15,220 km^2 and is spread over an elevation range of about 1570-6000 m above mean sea level (amsl) (Alam et al. 2015). Kashmir Valley forms a part of the Jhelum basin and has a well-developed drainage system. The Jhelum Basin lies between 32°58'42" to 35°08'02" north latitude and 73°23'32" to 75°35'57" east longitude and is mostly confined within the Kashmir Valley. River Jhelum is a major tributary of river Indus and forms the lifeline of Kashmir Valley. It emerges from a spring at Verinag in South Kashmir and flows north to Wular Lake and finally down south-westwards to Uri and Muzzafarabad. After emerging from Wular lake, the river is referred to as the outfall channel (OFC), which serves the purpose of draining floodwaters from the lake. The Jhelum river system drains the entire valley and ultimately passes along the western boundary of Kashmir into Pakistan. The total length of the river Jhelum from Verinag to Uri is 239 km (Wani et al. 2019). It has a well-established meandering form and is sluggish in its course. The approximate width of the river is 350 feet at Sangam, 250 feet at Ram Munshi Bagh and 692 feet at Asham.

The Jhelum river system is fed both by rain and snow. Jhelum basin includes 24 catchments with the left bank tributaries draining the slopes of the Pir Panjal range, while the right bank tributaries come from the Himalayan slopes. A stream draining from Dal lake joins the river before it enters the principal city of Srinagar. A flood spill channel at Padshahi Bagh in Srinagar diverts high flood discharge to the low-lying areas on the left bank of river Jhelum. The channel has a total length of 44 km and functions only when the discharge in the river rises above the danger mark.

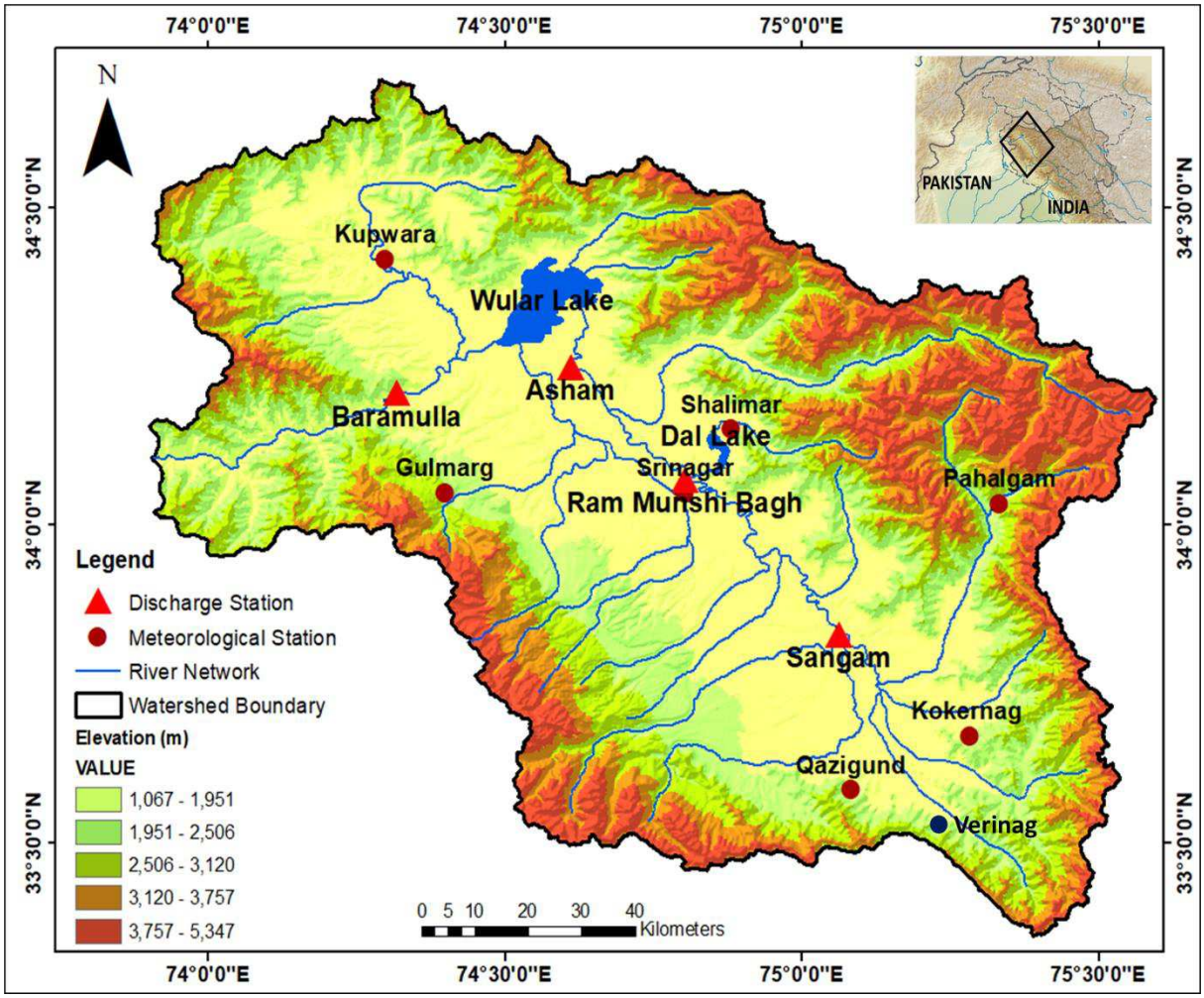

Fig. 1 Location map of Kashmir valley showing the elevation zones, Jhelum river network, meteorological stations and discharge stations.

The enclosure of Kashmir valley within high mountain ranges imparts it a distinct character having its peculiarities concerning the climate. Climate of the valley is a Mediterranean type, having a distinct seasonality. A year is divided into four seasons: winter (December to February), spring (March to May), summer (June to August), and autumn (September to November). The variation in annual temperature is high, ranging from -10 °C in winter to 35 °C in summer (Khattak et al. 2011; Rashid et al. 2015). The mean annual precipitation of the valley is 840 mm (Ahmad et al. 2017). Precipitation is dominated by snowfall occurring during winter, while rainfall occurs erratically for the rest of the year.

2.2. Data Collection, Analysis and Processing

Data is the most vital component of advanced hydrologic modelling and forecasting. The performance of model simulations is significantly affected by the availability and quality of geospatial, meteorological hydrological data records (Sugiura et al. 2016). In this section,

collection, analysis and processing of different datasets required as input for the model have been discussed.

2.2.1. Topography Data

The surface topographical information was extracted from 1 arc-second (30m) Shuttle Radar Topography Mission Digital Elevation Model (SRTM-DEM). Catchment boundaries and river networks were extracted from the DEM using D8 method of Esri software Arc-GIS 10.2. Keeping in view the limitations of SRTM DEMs (Schumann and Bates 2018), the delineated catchment boundaries and river networks were corrected using two references namely, Google Earth images and Watershed Atlas of India. The atlas provides the hydrological information of watersheds on a scale of 1:50000 (Central Water Commission (CWC) and National Remote Sensing Centre (NRSC) 2014).

2.2.2. Meteorological Data

Daily precipitation, maximum temperature and minimum temperature data for seven meteorological stations were collected from the Regional Meteorological Centre (RMC) Srinagar of India Meteorological Department (IMD) and Agro-meteorological Field Unit (AMFU) Srinagar. Evaporation data is recorded by AMFU Srinagar at Shalimar. Fig. 1 shows the spatial distribution of the meteorological stations in the study area. The geographic and other necessary information about these stations is summarized in Table 1. Substantial gaps in data were filled by using the multiple linear regression method of gap filling. Arithmetic average (AA), normal ratio (NR), and inverse distance (reciprocal-distance) weighting method (IDWM) and multiple linear regression (MLR) methods were used for gap filling (Kashani and Dinpashoh 2012). The best-fit method was selected based on the least root-mean-square error (RMSE) and the highest coefficient of correlation (r). These metrics are explained in Appendix A.

Table 1 Details of meteorological stations used for the study.

Station	Latitude	Longitude	Elevation (m)	Annual Precipitation (mm)	Mean Annual Temperature (°C)
Gulmarg	34° 03'	74° 24'	2705	1440	7.1
Kokernag	33° 40'	75° 17'	1920	1050	12.5
Kupwara	34° 25'	74° 18'	1609	1074	13.4
Pahalgam	34° 02'	75° 20'	2310	1276	10.0

Qazigund	33° 35'	75° 05'	1690	1212	13.0
Shalimar	34° 09'	74° 53'	1605	885	13.2
Srinagar	34° 03'	74° 50'	1588	744	13.9

MLR gave the least values of RMSE and the highest values of r. An average "r" of 0.93 and RMSE 4.54 for precipitation was obtained. For average temperature, these values were 0.98 and 1.44, respectively. At each station, 10% of the data was assumed to be missing, which was used for testing purpose (Sattari et al. 2017). The statistics were computed for the years 2001-2014. Inconsistencies in precipitation and temperature data at a station were evaluated using double mass curve analysis. The data were consistent, reflecting that the data was suitable for applying in hydrological modelling (Dike and Tilburg 2007).

2.2.3. Satellite Rainfall Data

Precipitation estimates are required for the development of flood forecasting and early warning system. The estimated or forecasted precipitation from numerical weather prediction modelling systems and satellite products is beneficial, especially for scarcely gauged catchments like Jhelum. In this study, forecasted precipitation and temperature data provided by the Climate Forecasting Application Network, output from the European Center for Medium-Range Weather Forecast (ECMWF) was used to increase the lead time of forecast. ECMWF has the most extensive data archival system in the world and can provide weather forecasts for up to two weeks in advance (Asghar et al. 2019). ERA5 is the fifth-generation global atmospheric reanalysis produced by ECMWF. It covers the entire globe from 1 January 1979 and now produces near real-time data as well. It has a horizontal spatial resolution of 0.25˚×0.25˚and a temporal resolution of 1 hour. The ERA5 precipitation data was verified with ground observation data at all the seven rainfall stations of IMD for the years 2010-2014.

Gridded precipitation and temperature data for each station was interpolated by inverse distance method (IDW) for obtaining the precipitation the station. For evaluating the accuracy of the ERA5 precipitation against ground observation data, these datasets were aggregated into daily timescales. ECMWF data was initially corrected using a standard procedure derived from the difference between monthly observed and satellite data (He et al. 2017). Verification of corrected satellite data was performed using yes/no dichotomous verification and statistical measures, namely RMSE, r and Mean error (ME) (Casati et al. 2008). Correlation coefficient of temperature data exhibited correlation coefficient (r) in the range of 0.93-0.95. The yes/no-dichotomous verification showed values between 0.72-0.80 (perfect value is 1) for various

stations. Probability of detection (POD) for various stations ranged from 0.77-0.9 (perfect value is 1) and False Alarm Ratio (FAR) values were between 0.23-0.41. Thus, corrected ECMWF data was used for enhancing the lead time of forecast.

2.2.4. Hydrological Data

The observed discharge and gauge measurements at four principal gauging sites of river Jhelum system were obtained from the Planning and Design Division of Irrigation and Flood Control (IFC) Department, Kashmir. Fig. 1 shows the location of the selected gauging stations and the details are listed in Table 2. The discharge and gauge (water level) data at these stations was analysed for the period 2001-2014.

Table 2 Location and hydrological characteristics of discharge stations of River Jhelum.

Station	Latitude	Longitude	Catchment Area (km^2)	Minimum Discharge (cumecs)	Maximum Discharge (cumecs)
Sangam	33° 50'	75° 4'	3731	12	3263
Ram Munshi Bagh	34° 4'	74° 48'	5490	16	2055
Asham	34° 15'	74° 37'	7485	26	1348
Baramulla	34° 12'	74° 19'	13604	16	1467

Double mass curve analysis was used to check the consistency of data records at all the stations. Both discharge and gauge data were consistent and thus appropriate for building the hydrological model of the basin. The department records gauge data daily while the discharge data is mostly recorded at an interval of 2-3 days. A gauge-discharge relation at each station was thus computed for model calibration and validation. Rating curves at flood discharge sites also serves as the downstream boundary condition for the hydrodynamic model. The relationship between the stage and the discharge for rivers is generally expressed in terms of a single-valued relation given in Equation (1).

$$Q = C(G - a)^N \quad (1)$$

Where Q is the discharge, G is the gauge height (stage), a is a constant which represents the gauge reading corresponding to zero discharge, C and N are rating curve constants. For each station, the parameters a, C and N were calibrated using historical stage and discharge values in order to obtain the best-fit equation. The rating curves for each gauging site are given in

247 Table 3. Statistical indices, namely r and RMSE were used to validate the rating curves at each
248 station (Table 3).

249 **Table 3 Gauge discharge relations at various gauging stations used for gap filling.**

S. No.	Station	R.L of zero gauge (m)	G-Q Equation	r	RMSE
1	Sangam	1584.80	$Q = 0.068(G - 1584.60)^{4.136}$	0.97	22.57
2	Ram Munshi Bagh	1580.14	$Q = 1.622(G - 1577.58)^{2.867}$	0.98	16.26
3	Asham	1576.22	$Q = 0.150(G - 1572.56)^{4.067}$	0.96	28.34
4	Baramulla	1572.15	$Q = 10.284(G - 1569.65)^{2.377}$	0.96	24.07

250 **2.2.5. River Cross Section Data**

251 Channel and flood cross sections of the plain give the topographical description of the basin to
252 be modelled. These lie approximately perpendicular to the direction of flow. The measured
253 cross-sections for the trunk river and its tributaries were obtained from IFC Department,
254 Kashmir. The cross sections of the floodplains were extracted from the SRTM DEM of the
255 basin.

256 **3. Methodology**

257 MIKE 11 model was used to develop a flood forecasting system for river Jhelum. This model
258 has been used for solving various problems of water resources planning and management (Khu
259 et al. 2001; Thompson et al. 2004; Doulgeris et al. 2011). For this purpose, MIKE 11 has several
260 modules like advection-dispersion (AD), ECO Lab (water quality modelling), data assimilation
261 (DA), flood forecasting (FF), hydrodynamic (HD), rainfall-runoff (RR) and ice modelling. The
262 present study uses MIKE 11 NAM, HD and FF modules for rainfall-runoff simulation,
263 computation of floods flows and increasing the forecast lead time for river Jhelum in Kashmir
264 Valley. A flowchart showing various steps in the development of the flood forecasting system
265 is illustrated in Fig.2.

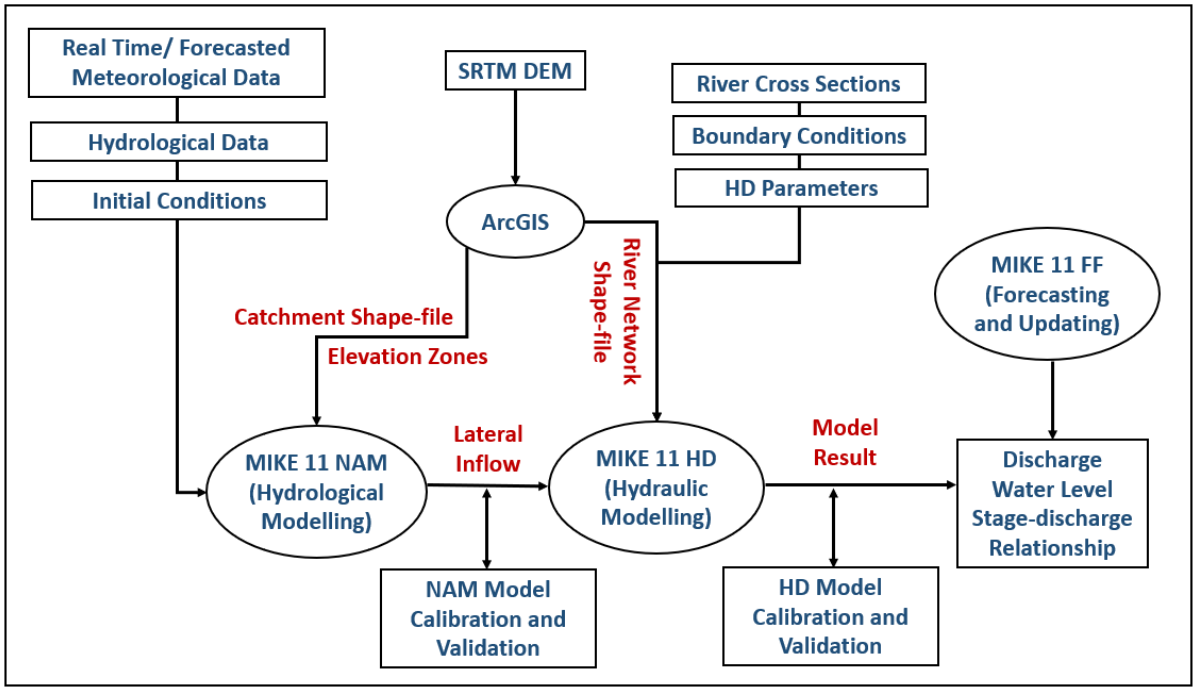

Fig. 2 Flowchart for development of the flood forecasting system for Jhelum basin.

A method for flood forecasting was developed using forecasted precipitation data and different modules of MIKE 11 software. The complete drainage area of the valley was modelled with a lumped, conceptual hydrologic model, MIKE 11 NAM and then integrated to 1-D hydrodynamic model, MIKE 11 HD for routing the flow through the river network. The modules were calibrated and validated using historical hydro-meteorological data to increase the lead time and accuracy of flood forecasts. MIKE 11 NAM and HD modules require morphometric characteristics of the catchment as inputs. These include catchment boundaries, river networks and river cross-sections. These were extracted from the 1 arc-second (30 m) SRTM DEM of the river basin. MIKE 11 NAM and HD models were calibrated and validated using observed hydro-meteorological data. Forecasted precipitation and temperature data provided by the European Centre for Medium-Range Weather Forecast (ECMWF) was used to increase the lead time of forecast to 7 days. The accuracy of forecasts was improved by using MIKE 11 FF module. Results were assessed by the comparison of observed and predicted discharge hydrographs of River Jhelum.

3.1. Hydrologic Modelling-Application of MIKE 11 NAM

NAM model was initially established by Nielsen and Hansen of the Technical University of Denmark (Nielson and Hansen 1973) and has been both revised and employed broadly by the Danish Hydraulic Institute. Structurally, the model is a reproduction of the land phase of the

286 water cycle. NAM considers four different but mutually inter-related storages, which serve as
287 various physical components of the catchment. These storage components, shown in Fig. 3. are
288 snow storage, surface storage, lower or root zone storage, and groundwater storage. NAM
289 simulates the precipitation-discharge processes by constantly computing the water content in
290 these storage components. NAM generates catchment runoff from precipitation using
291 information of temporal changes in evapotranspiration, soil moisture content, groundwater
292 recharge, and groundwater levels. The resultant catchment discharge is conceptually
293 subdivided into overland flow, interflow, and base flow components.

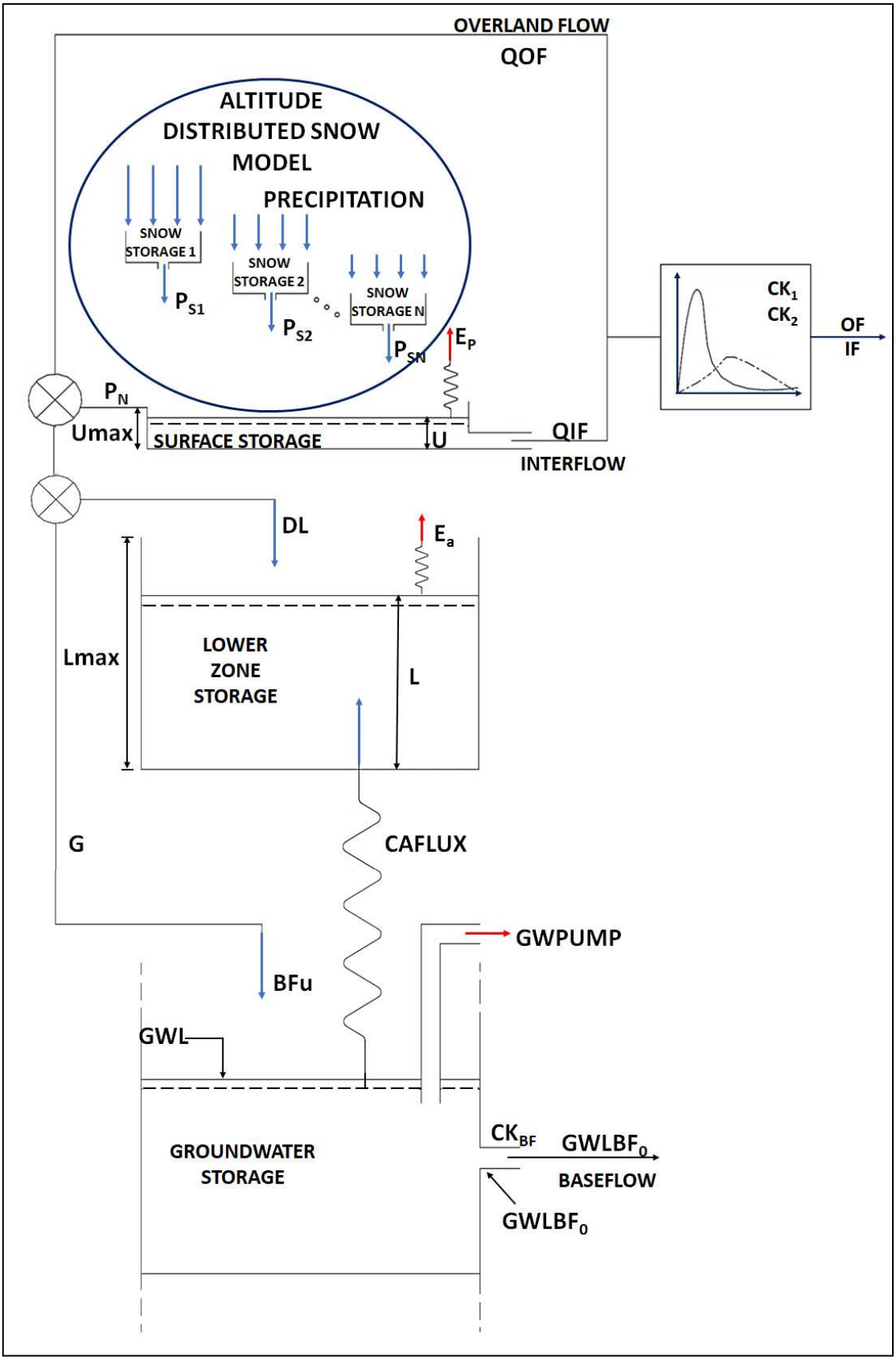

294

295 **Fig. 3 Structure of the NAM model showing the extended altitude distributed snow**

296 **model.**

From a technical viewpoint, NAM is a 1-dimensional, deterministic, lumped, conceptual, rainfall-runoff module of MIKE 11. It has moderate input data requirements and is based on physical structures and semi-empirical equations (DHI 2017). The values of the model parameters are specified for the complete catchment and some of them can be derived from the physiography, climate and soil characteristics of the catchment. Nevertheless, to determine the final parameter values, the model is calibrated against a time series of hydrological measurements. Model calibration is achieved manually (trial-and-error method) or through automatic computer-based operations (Kan et al. 2019).

MIKE 11 NAM uses nine parameters to represent various surface zone, root zone and groundwater storage. In event of applying snowmelt component, NAM module requires two extra snowmelt parameters. The model employs the temperature index model for the computing daily snowmelt. Snow melt module of NAM uses a temperature input time series, generally mean daily temperature and parameters for snow storage. These basic parameters are described in Table 4.

Table 4 Different parameters of surface zone, root zone, groundwater zone and snow storage of the NAM Model

Storage Component	Parameter	Unit	Typical Parameter Range	Description
Surface-root zone	U_{max}	mm	5-35	Maximum water content in surface storage
	L_{max}	mm	50-400	Maximum water content in lower zone/root storage
	CQOF	-	0-1	Overland flow Coefficient
	CKIF	h	200-2000	Time constant for interflow
	TOF	-	0-0.9	Root zone threshold value for overland flow
	CK_1	h	3-72	Timing constant for overland flow
	CK_2	h	3-72	Timing constant for interflow
	TIF	-	0-0.9	Root zone threshold value for interflow

Groundwater	TG	-	0-0.9	Root zone threshold value for groundwater recharge
	CK_{BF}	h	500-5000	Timing constant for base flow
Extended Groundwater	C_{qlow}	-	0-100	Lower baseflow/recharge to lower reservoir
	C_{klow}	h	1000-30000	Time constant for routing lower baseflow
Snow melt	C_{SNOW}	mm/°C/day	-	Degree-day coefficient
	T_0	°C	-	Base Temperature

Using precipitation, potential evaporation and temperature as input, the model simulates: Snow accumulation and melting, interception, evapotranspiration, overland flow, groundwater recharge and baseflow are calculated.

NAM Model Setup, Calibration and Validation

MIKE 11 NAM was set up using catchment boundaries and hydrometeorological data. Sub-catchment boundaries were delineated from 30-m SRTM of the basin using ArcGIS software. Entire Jhelum basin was divided into 18 sub-catchments based on the major tributaries draining them. Mean areal precipitation for each sub catchment was calculated using the Thiessen polygon method (Schumann 2006) and daily precipitation data from seven stations. The Thiessen polygons for each sub-catchment were obtained using rainfall-runoff editor of NAM model and are shown in Fig. 4. Mean temperature was calculated using the lapse rate approach. Lapse rate is defined as the rate of decrease of temperature with an increase in elevation conferring to a correlation that arises from the data from seven stations (Sheridan et al. 2010). The actual evapotranspiration is calculated by NAM model based on evaporation data and model parameters.

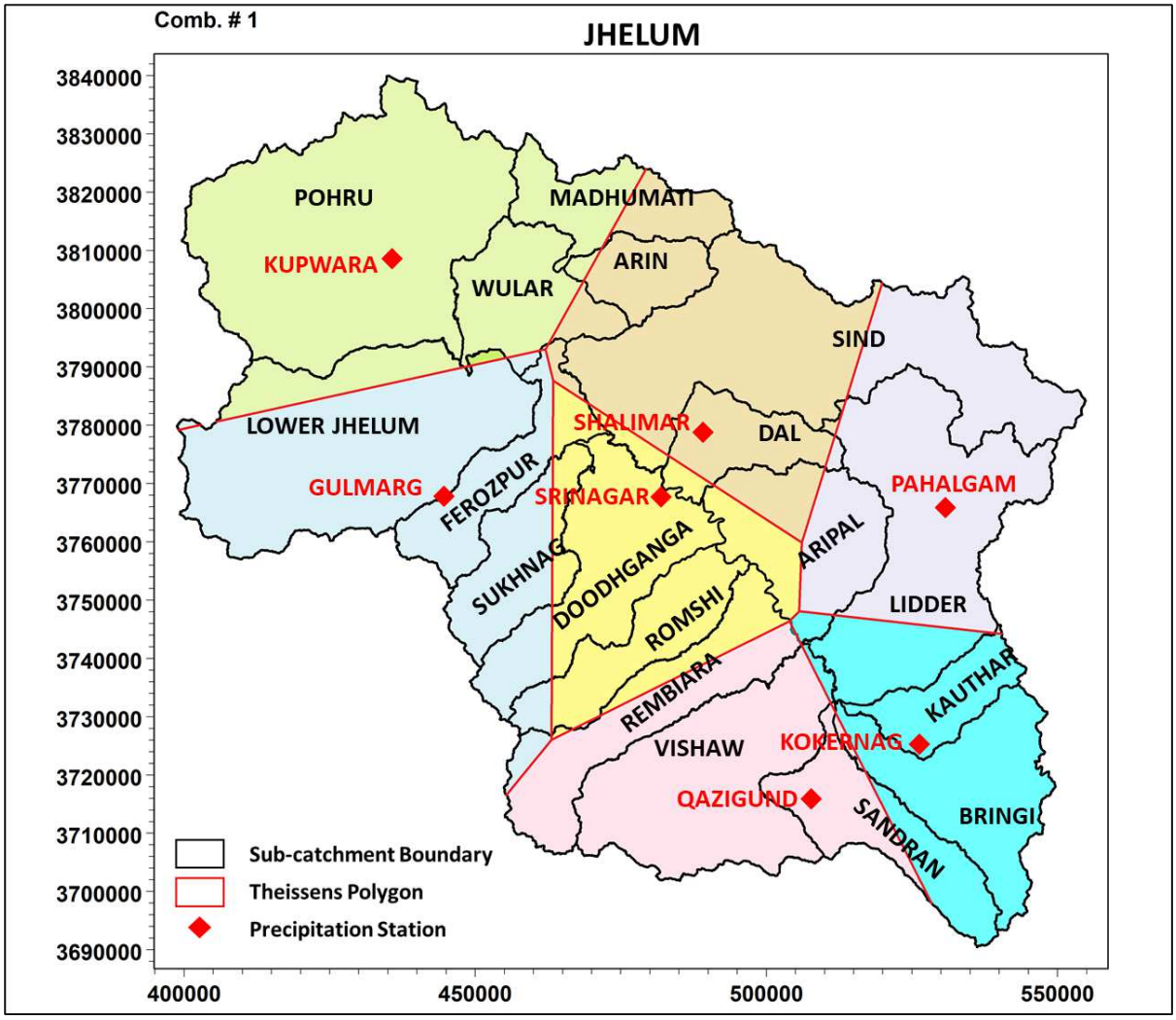

Fig. 4 Sub-catchments of Jhelum basin and Thiessen polygons of different rainfall stations.

(The axis units are UTM coordinates in meters)

MIKE 11-NAM model was applied to 18 sub-catchments of Jhelum River basin shown Fig. 4 to simulate rain and snowmelt-runoff at a daily time step for the years 2001-2008. The calibration procedure was based on three steps- first the setting up of surface-root zone, second the groundwater modules, and lastly the snow-melt module. At first, the NAM model was set up using the seven surface-root zone parameters and two groundwater parameters. Parameters for each sub-catchment were estimated using the auto-calibration routine of MIKE 11. The sub-catchments were calibrated against discharge available at four gauging stations on the river Jhelum for the calibration period, using the auto-calibration routine of MIKE 11 NAM. Auto-calibration for MIKE 11 NAM can be run to optimize four "objective functions" (Madsen 2000). These functions are:

1. agreement between the average simulated and observed catchment runoffs: overall volume error (%WBL);
2. overall agreement of the shape of the hydrograph: overall root mean square error (RMSE)
3. agreement of peak flows: average RMSE of peak flow events;
4. agreement of low flows: average RMSE of low flow events.

A combination of two or more of these objective functions can be selected for a particular study. Since the MIKE 11 NAM in this study is a component of flood forecasting system, overall volume error and peak flow RMSE were chosen.

A thorough examination of the hydrographs for the calibration period showed that runoff was significantly affected by snowfall. Precipitation during winters (December to February) had no to little impact on the observed runoff. Snow accumulates from December, especially in high altitude zones, and melts at a specific rate throughout the year to maintain river flow even during dry periods. Thus, an altitude distributed snow-melt module was also included in the model. Snow-melt module was calibrated manually, using temperature data and a trial-and-error method.

The initial conditions for the first run were set using rough estimates based on the subjective understanding of each sub-catchment. The model was run for the calibration period (2001-2008) starting from January 1st, 2001. Average simulated values of January 1st were taken as initial conditions for the second run, and this was repeated till the best values of initial conditions were found. For validating the NAM model, daily discharge predictions were made for the period, from 2009 to 2014 using the NAM parameters estimated during model calibration.

For interpreting the model results thoroughly, both graphical and statistical criteria must be looked at during the calibration and validation periods. For graphical comparisons, hydrographs of observed and simulated hydrographs are tested. The performance of the model after auto-calibration was determined by comparing observed and simulated discharges at each discharge station. Statistical characteristics include the objective functions of model calibration, i.e., overall water balance error (%WBL) and peak RMSE. The errors in model simulation were evaluated in terms of mean absolute error (MAE), p-bias, RMSE, peak error and the peak time error, while coefficient of determination (R^2) and the widely recognized Nash-Sutcliffe efficiency (NSE) (Nash and Sutcliffe 1970) gave the measures of model performance. These metrics are described in Appendix A. When the model performs

efficiently, %WBL, p-bias, MAE and RMSE values are close to zero and the values of R^2 and NSE are close to one. Models are tested separately for calibration and validation periods using the parameters obtained during calibration.

3.2. Hydrodynamic Modelling-Application of MIKE 11 HD

Hydrodynamic model, commonly identified as MIKE 11 HD is the core of MIKE modelling system. MIKE 11 HD is a one-dimensional, unsteady, non-uniform flow simulation model. It computes unsteady flow, discharge and water level in rivers and channels. MIKE 11 HD applies a one-dimensional, implicit, finite difference technique for the numerical solution of the Saint-Venant equations and can be defined as follows (DHI 2017):

$$\frac{\partial Q}{\partial x} + \frac{\partial A}{\partial t} = q \tag{2}$$

$$\frac{\partial Q}{\partial t} + \frac{\partial \left(\alpha \frac{Q^2}{A}\right)}{\partial x} + gA\frac{\partial h}{\partial x} + \frac{gQ|Q|}{C^2AR} = 0 \tag{3}$$

$$C = \frac{R^{1/6}}{n} = MR^{1/6} \tag{4}$$

Where,

Q = discharge (m^3/s);

A = cross section (flow) area (m^2);

q = lateral inflow (m^2/s);

h = water level above a reference datum (m);

x = downstream direction (m);

t = time (s);

n = Manning resistance coefficient ($sm^{-1/3}$);

C = Chezy coefficient ($m^{1/2}s^{-1}$)

M = Manning number ($m^{1/3}s^{-1}$)

R = the hydraulic or resistance radius (m);

g = acceleration due to gravity (m^2/s); and

α = momentum distribution coefficient.

α is introduced to account for the non-uniform vertical distribution of velocity in a section.

The computational grid of MIKE 11 HD encompasses alternating Q-points and h-points along the river. Discharge (Q) and water level (h) are computed at these points for every time step.

Based on the maximum distance, dx between two adjacent h-points, HD model auto-generates a computational grid. For the present study, the course of river Jhelum and 17 major tributaries were included in the HD model. Fig. 5 shows the Jhelum river network used for setting the HD model Maximum distance, dx, was set equal to 1000 m for the main river and the tributaries. The geometry of the river and its tributaries was established using various cross-sections and linear interpolation between them. Measured tributary cross sections were available at the head and tail of each tributary and at various important locations along the river length. Some cross sections were extracted from the SRTM DEM of the basin. Lakes were included in the HD model in the same manner as rivers, except as very wide and deep ones.

In addition to the natural drainage, a flood spill channel (FSC) at chainage 57068 m on river Jhelum in was included in the river network to reroute an excess flood discharge of Jhelum at Padshahi Bagh. The channel width varies from 91.5 m at head to 152 m at tail with a total reach of 44 km (Fig. 5). The channel finally drains into Wular Lake after collecting runoff from Doodhganga, Ferozpur and Sukhnag tributaries. River Jhelum flows in the form of streams till Sangam where major tributaries merge and Jhelum assumes the form of a river. The slopes of tributaries are steep while the main river form Sangam to Baramulla has a very gentle slope.

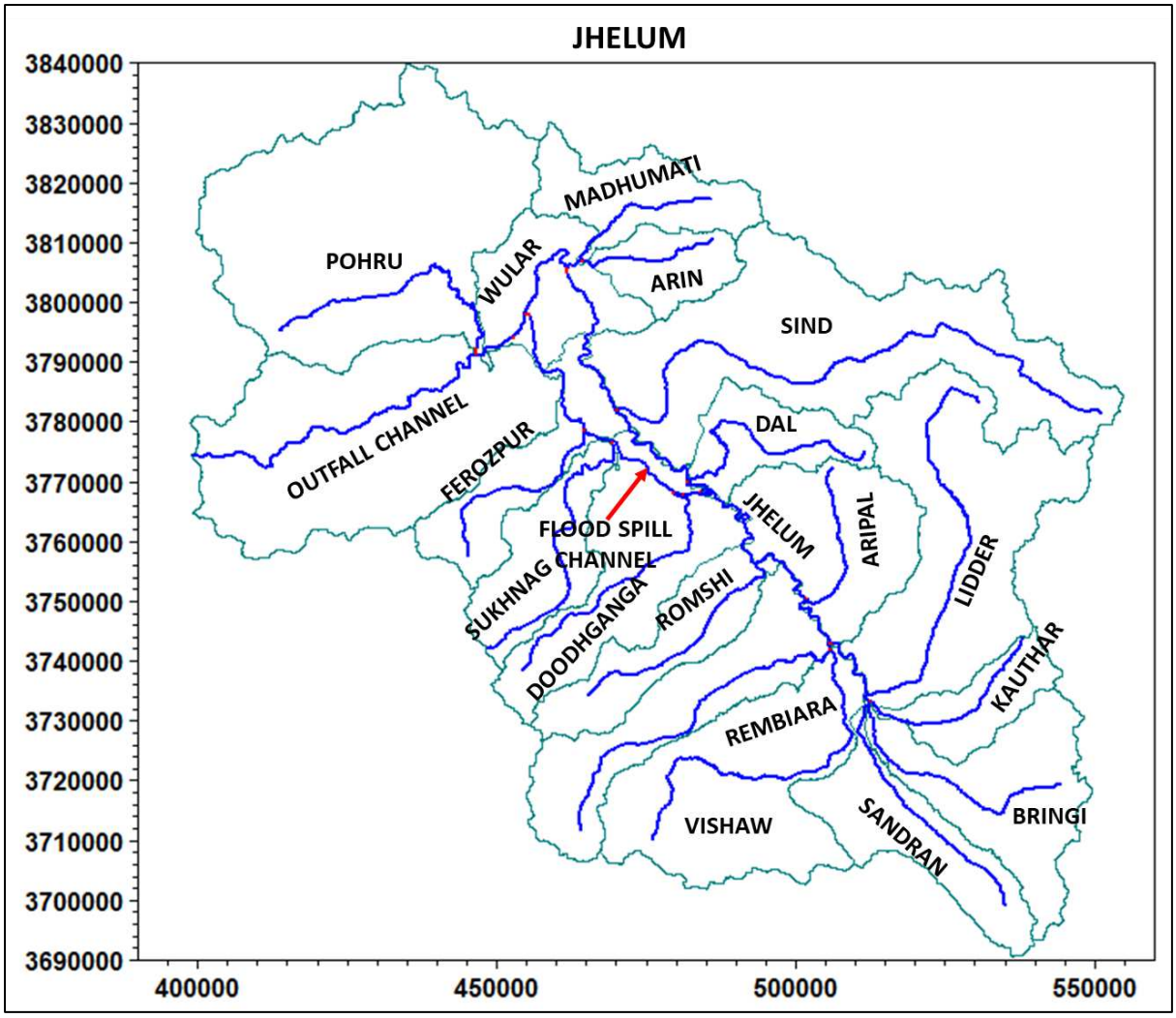

Fig. 5 Jhelum river network used for setting up MIKE 11 HD model.

(The axis units are UTM coordinates in meters)

Boundary conditions of the HD model depend on the data accessibility and physical state of the modelled area. Various boundary conditions can be used, for example reservoir supplied constant discharge, event-based hydrograph, a constant water level (for large water bodies), time-series of water level or a dependable gauge-discharge relationship of a gauging station. River Jhelum and its tributaries have their sources within the study area and do not have upstream gauge stations. The upstream boundary condition for each of these tributaries taken as an arbitrary constant discharge of $1 m^3/s$. The downstream boundary condition for river Jhelum was taken as the gauge-discharge (Q-h) relationship at the outlet. Global Manning number of $M = 20\ m^{1/3}/s$ and the Delta (Default Values) of 0.6 were used. Wave approximation of 'High Order Fully Dynamic' was considered to simulate the river system.

3.3. Integration of NAM and HD modules

The NAM model was linked with the HD model to input the lateral inflow from the catchments into the river channels (Fig. 5). The integrated model was simulated from January 2001 to December 2008. A fixed time step of one minute was selected for the integrated model. A larger timestep of simulation produced systematic violation of the Courant Number (i.e., CN>1), while smaller timesteps enhance the computational time substantially. The results of NAM model were taken as the initial conditions of rainfall-runoff, while for the HD model initial condition was the parameter file. Table 5 describes the reach lengths of various tributaries connected with their respective sub-catchments.

Table 5 Integration of sub-catchments for lateral flows in the river network

Sub-catchment	Area (km^2)	Tributary	Upstream (US) chainage (m)	Downstream (DS) chainage (m)
Arin	252	Arin	0	24932
Aripal	632	Aripal	0	29011
Bringi	670	Bringi	0	45915
Dal	334	Dal	0	49419
Doodhganga	750	Doodhganga	0	52671
Ferozpur	442	Ferozpur	0	39234
Kauthar	272	Kauthar	0	35713
Lidder	1256	Lidder	0	86579
Lower Jhelum	1505	Outfall Channel	0	75760
Madhumati	419	Madhumati	0	28139
Pohru	1842	Pohru	0	52766
Rembiara	687	Rembiara	0	64042
Romshi	440	Romshi	0	43010
Sandran	502	Sandran	0	48083
Sind	1661	Sind	0	110000
Sukhnag	439	Sukhnag	0	54600
Vishaw	1032	Vishaw	0	70133
Wular	469	Wular	0	28339

The tributaries of Jhelum mostly originate in the mountains and follow a steep course before merging into the river. However, the main river flows with a very gentle slope from Sangam

427 to Baramulla. Thus, a high-order fully-dynamic wave approximation was used to simulate this
428 river system.

429 For the HD parameter file, the chief calibration parameter is the bed resistance. MIKE 11 HD
430 has two options for describing bed resistance: (1) Manning's and (2) Chezy's. manning's *M* is
431 the inverse of Manning's roughness coefficient (*n*) and is the same as Strickler coefficient. The
432 value of "*n*" ranges from 0.01 for smooth channels to 0.10 for densely vegetated channels. For
433 mountainous streams with cobble and stony beds, value of Manning's coefficient can be as
434 high as 0.07.

435 ***Calibration and Validation of Integrated NAM-HD Module***

436 The integrated NAM-HD module was calibrated based on the observed discharge at Sangam,
437 Ram Munshi Bagh, Asham and Baramulla stations. The time-period for calibration was 2001-
438 2008. For validation, the time period selected was 2009-2014. These time periods were selected
439 on the basis of availability and quality of data at the gauge stations. The simulated values of
440 discharge were compared with the observed values using several statistical indices (Appendix
441 A).

442 **3.4. Flood Forecasting-Application of MIKE 11 FF**

443 A classic issue in real time application of flood-forecasting models is that the simulated
444 discharge differs from the observed runoff at the time of forecast (Jonch-Clausen and Refsgaard
445 1984). With a view to get optimal benefit of the real time discharge measurements in the
446 forecasts, a kind of updating of the hydrological model is recommended before the forecast is
447 made (Refsgaard 1997). MIKE 11contains an automatic updating (data assimilation) routine,
448 MIKE 11 FF (Flood Forecasting) to improve the correctness of real-time measurements in
449 forecasts. It performs calculations needed to predict water level and discharge variations in
450 fluvial systems. The predictions are made on the basis of rainfall-runoff relations of the
451 catchments and inflow and outflow through model boundaries (DHI 2017).

452 The updating routine compares and analyses the simulated water levels and discharges to the
453 measured values prior to the time of forecast (ToF). A conceptual flowchart describing the
454 simulation time period for the forecasting procedure is shown in Fig. 6. ToF is defined relative
455 to the hindcast and forecast periods. The hindcast period defines the simulation period up to
456 the time of forecast, and is given in the simulation file.

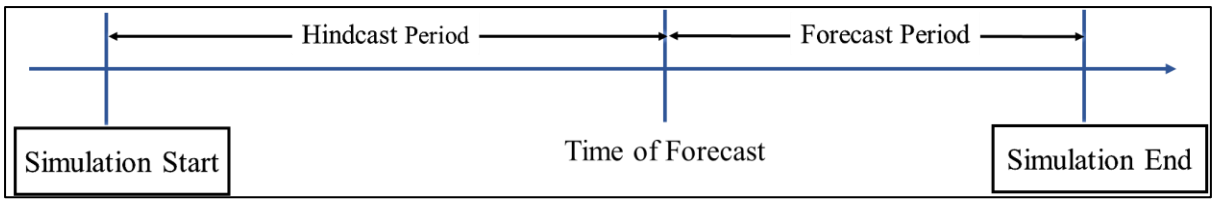

Fig. 6 Conceptual flowchart of simulation period in forecasting procedure

Precise boundary and rainfall forecasts, a well-calibrated model having suitable updating efficiency generate accurate forecasts. The FF module of MIKE 11 is an automatic real-time updating routine which minimizes two types of errors or deviations between observed and predicted data, namely amplitude error and phase error (Paudyal 2002). The updating procedure differentiates between the two error types and consequently makes corrections by minimizing the objective functions given as (Rafieeinasab et al. 2014):

$$\sum_{i=1}^{n}\left(F_i\left\{M_i-\left[S_i+A_e-\frac{S_i-S_{i+1}}{\Delta T}\times P_e\right]\right\}\right)^2$$

Where;

M = Measured discharge (m^3/s);

S = Simulated discharge (m^3/s);

A_e = Amplitude error (m^3/s);

P_e = Phase error (s);

n = Number of values included;

F = A weighted factor;

ΔT = Time step (s).

Update parameters are calibrated with the intention to correct distinction between deviations in time (phase errors) and deviations in volume (amplitude errors).

Flood Forecasting using the integrated NAM-HD Model with ECMWF Input

Forecasted rainfall and temperature data is required by the integrated model to forecast the flood with a sufficient lead time. The forecasted precipitation and temperature data of ECMWF for the years 2009-2014 was used in the study to generate forecasts with lead times up to 10 days. Model validation was carried out by comparison between observed and simulated flows at Sangam.

475 ***Updating using MIKE 11 FF***

476 The flood forecasting model developed using the MIKE 11 NAM and HD modules was
477 updated with the observed discharge values at various sites. Updating parameters identified by
478 DHI are max phase error, analysis period (AP), time constant in AP, time constant in forecast
479 period, adjust factor, alpha, and peak value. Max phase error and time constant in AP are
480 typically equal to AP. Values of AP, time constant in forecast period and alpha are established
481 by calibration. Adjust factor value is generally equal to 1, while the peak value is got from the
482 observed discharge hydrographs. The observed and simulated discharges are compared and
483 analysed in the hindcast period and the simulations are corrected to minimize the
484 inconsistencies between the observed data and model result.

485 **4. Results and Discussion**

486 **4.1. Calibration and Validation of NAM model**

487 MIKE 11-NAM model was calibrated for estimation of daily runoff for river Jhelum at four
488 principal gauging sites. During auto-calibration, the optimal values of various NAM parameters
489 were obtained. Overall % WBL values for Sangam, Ram Munshi Bagh, Asham and Baramulla
490 stations were -6.8%, 9.4%, 12.3% and 15.2%, respectively. Peak RMSE at these stations were
491 25 m^3s^{-1}, 38 m^3s^{-1}, 57 m^3s^{-1} and 69 m^3s^{-1}. The values of objective functions, i.e., % WBL and
492 peak RMSE suggest the NAM model has been calibrated adequately. A set of NAM model
493 parameters was identified to represent various sub-catchments of the basin. The values of NAM
494 parameters for each sub catchment obtained after calibration are given in Table 6.

Table 6 Final values of NAM parameters and initial conditions obtained by model calibration (2001-2008).

Sub-catchment	Area (km^2)	Initial Conditions					Surface-Rootzone							Groundwater		Snowmelt	
		U	L	QOF	QIF	BF	Umax	Lmax	CQOF	CKIF	CK1,2	TOF	TIF	TG	CKBF	Csnow	T0
Sandran	502	0.72	0.87	0.61	0.8	2.5	10.8	161	0.57	772	39.90	0.756	0.627	0.623	4148	1	6
Bringi	670	0.85	0.73	0.59	0.92	3	8.7	131	0.61	750	24.70	0.715	0.608	0.873	4020	1	6
Kauthar	272	0.66	0.73	0.65	0.82	2	10.6	143	0.64	692	16.60	0.82	0.887	0.923	3833	2	4
Lidder	1256	0.75	0.88	0.72	0.76	6.25	10.1	135	0.64	756	38.50	0.792	0.658	0.566	3239	1	6
Vishaw	1032	0.78	0.8	0.51	0.86	5.5	9.5	150	0.6	760	29.50	0.75	0.589	0.541	4303	1	6
Aripal	632	0.88	0.76	0.52	0.9	2.75	14.7	169	0.38	780	30.70	0.922	0.41	0.899	4211	2	4
Rembiara	687	0.85	0.89	0.65	0.77	2.5	10.1	158	0.52	749	21.60	0.484	0.702	0.851	3039	2	4
Romshi	440	0.73	0.86	0.62	0.92	2.5	10	144	0.55	672	40.80	0.891	0.481	0.797	2257	1	4
Sind	1661	0.65	0.79	0.78	0.8	6.25	11.7	161	0.51	663	11.20	0.867	0.846	0.937	2007	1	4
Dal	334	0.67	0.84	0.5	0.84	5.5	12.1	148	0.54	715	11.40	0.619	0.844	0.743	3995	1	4
Doodhganga	750	0.89	0.71	0.59	0.92	3.25	13.3	193	0.43	699	40.80	0.875	0.584	0.945	2998	1	4
Sukhnag	439	0.79	0.77	0.73	0.81	3.75	12	140	0.45	699	26.40	0.937	0.419	0.804	2599	1	4
Ferozpur	442	0.6	0.85	0.51	0.83	3.5	11.1	150	0.49	791	12.50	0.744	0.49	0.505	2672	1	4
Arin	252	0.6	0.7	0.67	0.63	2.75	14.2	183	0.46	712	34.50	0.695	0.675	0.774	3187	1	4
Madhumati	419	0.6	0.88	0.54	0.89	2.75	12.6	163	0.54	656	29.60	0.603	0.543	0.599	3417	1	4
Pohru	1842	0.76	0.8	0.81	0.79	3.25	13.2	190	0.49	705	18.30	0.534	0.436	0.639	3322	1	4
Wular	469	0.69	0.76	0.66	0.65	5.5	12.8	183	0.37	785	28.00	0.611	0.689	0.521	3267	1	4
Lower Jhelum	1505	0.7	0.78	0.72	0.84	7.5	13.5	175	0.42	760	31.40	0.475	0.786	0.552	3122	1	4

Model performance after calibration was judged by graphical comparison between observed and simulated discharge values. A graphical assessment of the MIKE 11-NAM model results, for calibration period (2001-2008) for stations Sangam, Ram Munshi Bagh, Asham and Baramulla, is shown in Fig. 7. It is observed from the figure that NAM model simulates runoff peaks and their date of occurrence precisely. Low flows, particularly in winter season, are also modelled well by the calibrated model. The calibrated NAM model was validated using the data for the period 2009-2014. Performance of NAM model during calibration and validation periods was evaluated in terms of various indices listed in Table 7. The values suggest that the NAM model reasonably simulates the observed discharge in most conditions. A positive p-bias values for Ram Munshi Bagh, Asham and Baramulla stations indicate that the flow is overestimated, which is also reflected in the positive %WBL values at these stations. Values of r, RMSE and NSE also indicate good performance of the models both during calibration and validation periods. This means that the models do not exhibit any bias towards the calibration period. Thus, the developed model can be used satisfactorily for any simulation period (Ahmed 2010).

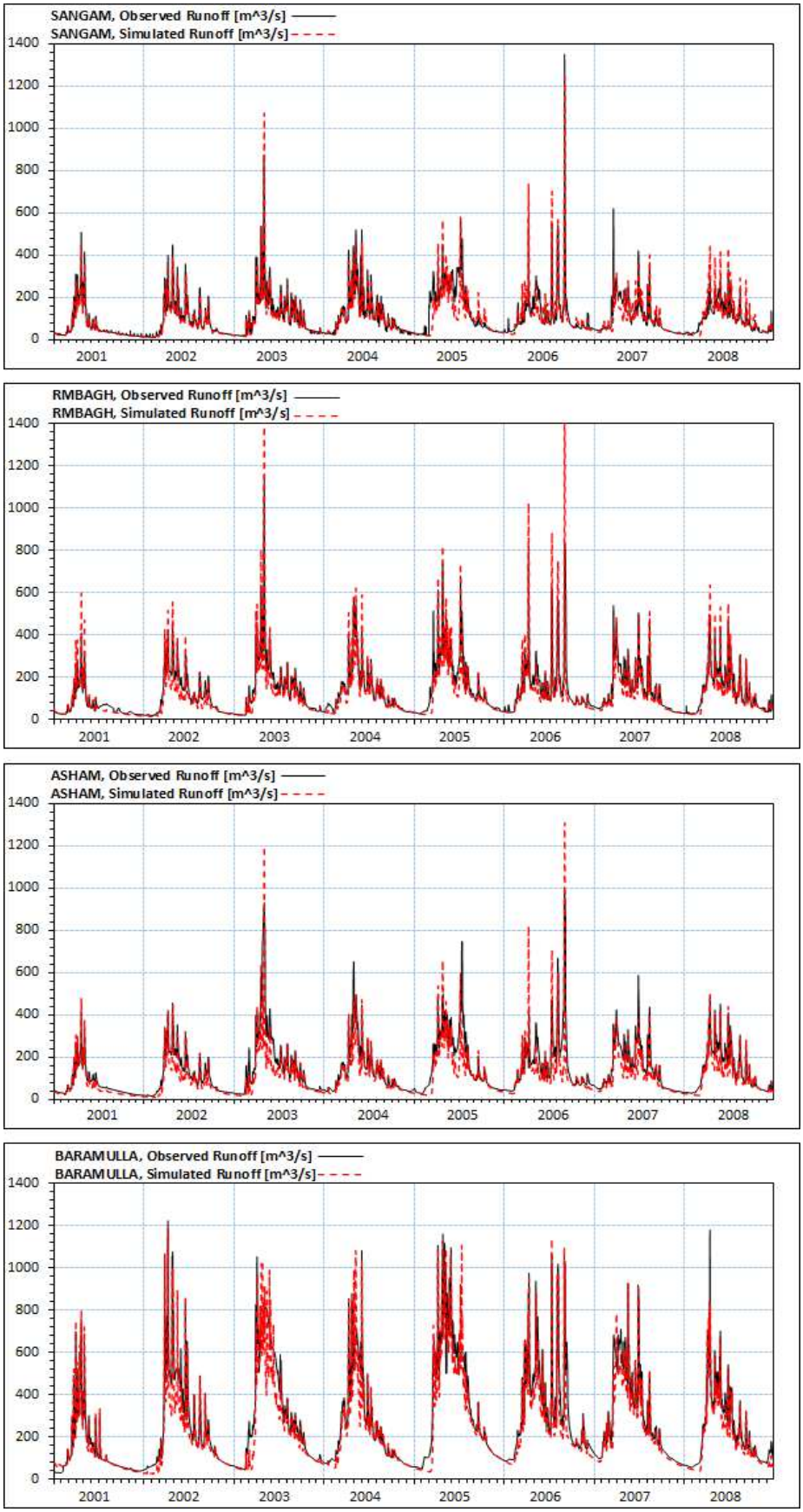

Fig. 7 Time series plots of observed and simulated data at various stations for calibration period (2001-2008).

Table 7 Performance indicators of NAM model during calibration (2001-2008) and validation (2009-2014) periods.

Performance Indicator	Calibration				Validation			
	Sangam	Ram Munshi Bagh	Asham	Baramulla	Sangam	Ram Munshi Bagh	Asham	Baramulla
R^2	0.72	0.75	0.73	0.77	0.78	0.71	0.72	0.73
MAE (m^3s^{-1})	3.79	2.98	4.01	4.97	2.9	4.8	4.7	5.3
NSE	0.69	0.7	0.7	0.72	0.72	0.69	0.71	0.72
p-bias (%)	-8.66	7.6	8.21	9.56	-7.73	9.88	8.96	9.88
RMSE (m^3s^{-1})	5.1	5.4	6.32	11.32	10.2	15.4	11.3	12.5
Peak Error (%)	5.6	7.8	8.5	7.6	6.8	10.2	11.2	10.5
Peak Time Error (h)	3.0	3.0	2.0	3.0	2.0	3.0	2.0	2.0

Heavy rainfall events lead to extensive overland flow and give rise to peak discharge events. Simulation of peak volumes was corrected by varying CQOF. Higher values of Umax and Lmax produced higher evapotranspiration rates and were adjusted accordingly (Doulgeris *et al.*, 2012). The basin has a snow-dominated runoff regime, i.e., snowmelt forms an essential component of the discharge in the basin. Snowmelt runoff increases during spring and reduces substantially during late summer. During the calibration and validation of the MIKE 11 NAM, it is observable that there is a modest agreement between the simulated values and the observed values. Shape and time of occurrence of peak of observed and simulated peak flows are almost identical. Peak values in the hydrographs are thus fairly well estimated. The model can precisely reproduce high flows.

4.2. Calibration and Validation of integrated NAM-HD model

For calibrating the bed resistance of various tributaries and main channel, several simulation runs were performed using observed discharge at various stations. For this purpose, years 2001-2008 were considered. Calibrated values of Manning's roughness coefficient "*n*" for the main river and its tributaries are given in Table 8.

534 **Table 8 Calibrated values of Manning's *n* or *M* for River Jhelum and its tributaries.**

Name	Chainage (m)	Manning's *M*	Manning's *n*
Arin	0-24932	17	0.059
Aripal	0-29011	22	0.045
Bringi	0-45915	19	0.053
Dal	0-49419	25	0.040
Doodhganga	0-52671	22	0.045
Ferozpur	0-39234	21	0.048
Flood Spillway Channel	0-48530	22	0.045
Jhelum	0-120000	22	0.045
Kauthar	0-35713	21	0.048
Lidder	0-86579	18	0.056
Madhumati	0-28139	19	0.053
Out Fall Channel	0-75760	22	0.045
Pohru	0-52766	20	0.050
Rembiara	0-64042	20	0.050
Romshi	0-43010	18	0.056
Sandran	0-48083	19	0.053
Sind	0-110000	19	0.053
Sukhnag	0-54600	18	0.056
Vishaw	0-70133	17	0.059
Wular	0-28339	20	0.050

535 Model validation was performed discharge data at the gauging stations for the period 2009-
536 2014. The time series plots for model validation corresponding to the observed discharge at
537 various stations are shown in Fig 8. Various statistical indices for evaluating the performance
538 of the integrated model are presented in Table 9. The errors in NAM model calibration may
539 result from uncertainties in input meteorological data or errors in calibration of NAM
540 parameters. Some errors in rainfall-runoff simulation can also be attributed to the fact that the
541 discharge measurements at various gauge stations are not regular and that gauge discharge
542 relations were used to fill a considerable amount of missing data. Errors in HD model can be
543 due to use of recorded cross sections of the river during the year 2018. Since river Jhelum is an
544 alluvium-based river, the cross sections keep changing regularly. The overestimation of flows
545 at Ram Munshi Bagh, Asham and Baramulla stations was also corrected to a significant extent.

546 This is because of diversion of excess flow to flood spill channel before Ram Munshi Bagh
547 station and inclusion of lake sections and flood storages in HD model. Most errors were
548 reduced to a great extent by using the integrated NAM-HD model as presented in Table 10.
549 The results can be further improved by implementation of modern measurement systems,
550 continuous record of the real-time meteorological and discharge data, improved frequency of
551 discharge measurements, river cross-sections update. Finer resolution data can help in more
552 accurate tuning of MIKE 11 NAM and HD parameters and thus improve the present results.

553

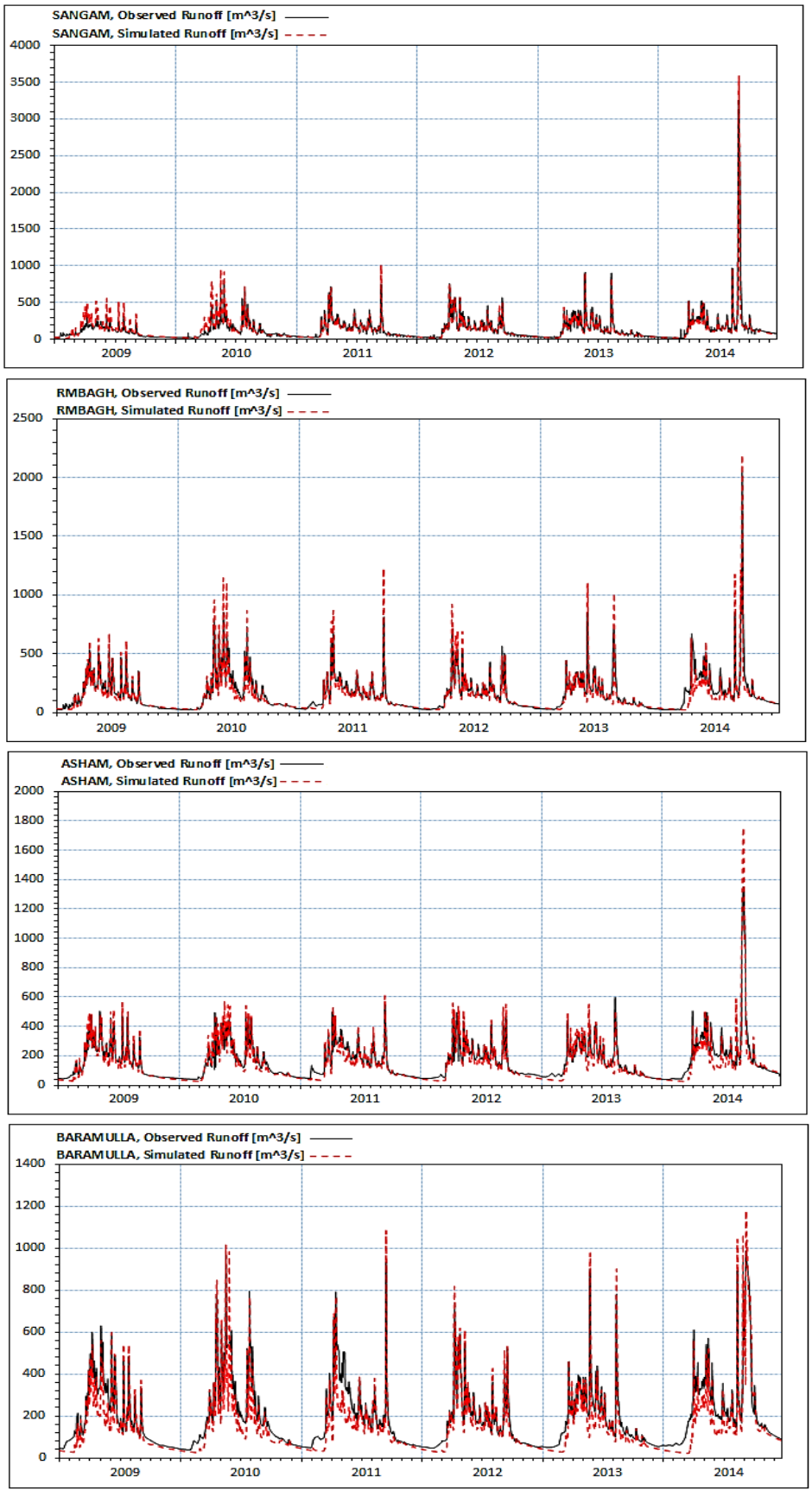

Fig. 8 Time series plots of simulated versus observed discharge values at various discharge stations of river Jhelum for validation period (2009-2014).

557 **Table 9 Performance indicators of integrated NAM-HD model during calibration (2000-2008)**
558 **and validation (2009-2014) periods.**

Performance Indicator	Calibration				Validation			
	Sangam	Ram Munshi Bagh	Asham	Baramulla	Sangam	Ram Munshi Bagh	Asham	Baramulla
R^2	0.81	0.86	0.81	0.84	0.87	0.83	0.82	0.80
MAE (m^3s^{-1})	2.88	2.12	3.25	3.68	2.12	4.08	3.01	4.13
NSE	0.78	0.77	0.80	0.81	0.79	0.78	0.77	0.82
p-bias (%)	-8.23	6.20	5.30	4.40	-7.11	5.20	4.60	4.10
RMSE (m^3s^{-1})	3.96	4.06	5.66	9.47	6.86	9.26	8.17	7.83
Peak Error (%)	7.85	5.48	6.09	4.92	4.77	7.71	9.06	8.38
Peak Time Error (h)	0.15	0.25	0.25	0.20	0.15	0.25	0.25	0.20

559 **Table 10 Percentage improvement of NAM model results during calibration (2000-2008) and**
560 **validation (2009-2014) periods by integrating the HD and NAM modules.**

Performance Indicator	Calibration				Validation			
	Sangam	Ram Munshi Bagh	Asham	Baramulla	Sangam	Ram Munshi Bagh	Asham	Baramulla
R^2	12.80	14.90	10.80	9.20	12.10	8.80	13.60	9.10
MAE	24.00	29.00	19.00	26.00	27.00	15.00	36.00	22.00
NSE	10.80	9.40	14.30	13.10	9.10	13.10	8.00	14.20
p-bias	5.00	18.42	35.44	53.97	8.00	47.37	48.66	58.50
RMSE	22.30	24.90	10.50	16.30	32.70	39.90	27.70	37.40
Peak Error	23.80	29.80	28.40	35.30	29.90	24.40	19.10	20.20
Peak Time Error	87.50	75.00	87.50	93.33	87.50	75.00	87.50	93.33

561 ### 4.3. Flood Forecasting using integrated NAM-HD model with ECMWF input

562 NAM-HD setup is evaluated for discharge forecasting at the Sangam gauge station using model
563 initial conditions and ECMWF forecasted temperature and precipitation data. For testing the
564 ability of the NAM-HD model for extended lead time forecasts, the model was run up to 10-
565 days lead time forecasts of ECMWF ERA5 for the years 2009-2014. The corresponding
566 performance measures by the NAM-HD model at 1 to 10 days forecast lead-times are

illustrated in Fig. 9. It is evident from Fig. 9 that even though the values of R^2 and NSE do not decrease considerably up to 10-days lead time, p-bias and MAE are acceptable only up to lead time of 8 days. However, for higher efficiency (NSE>7), the model may be applied for a maximum lead time of 7 days. The values of peak error and peak time error also increase considerably after 7 days lead time. Although the results confirm that the satellite-based ECMWF precipitation can be appropriately employed to run MIKE 11 NAM-HD model for flood prediction purpose in Jhelum basin, complete accomplishment of the potential of smooth satellite-based precipitation estimates calls for better analysis of optimal calibration procedure for incorporating remote sensing data into a real-time hydrological modelling system for vast ungauged or scarcely gauged basins of the world (Kong et al. 2019; Jiang and Wang 2019).

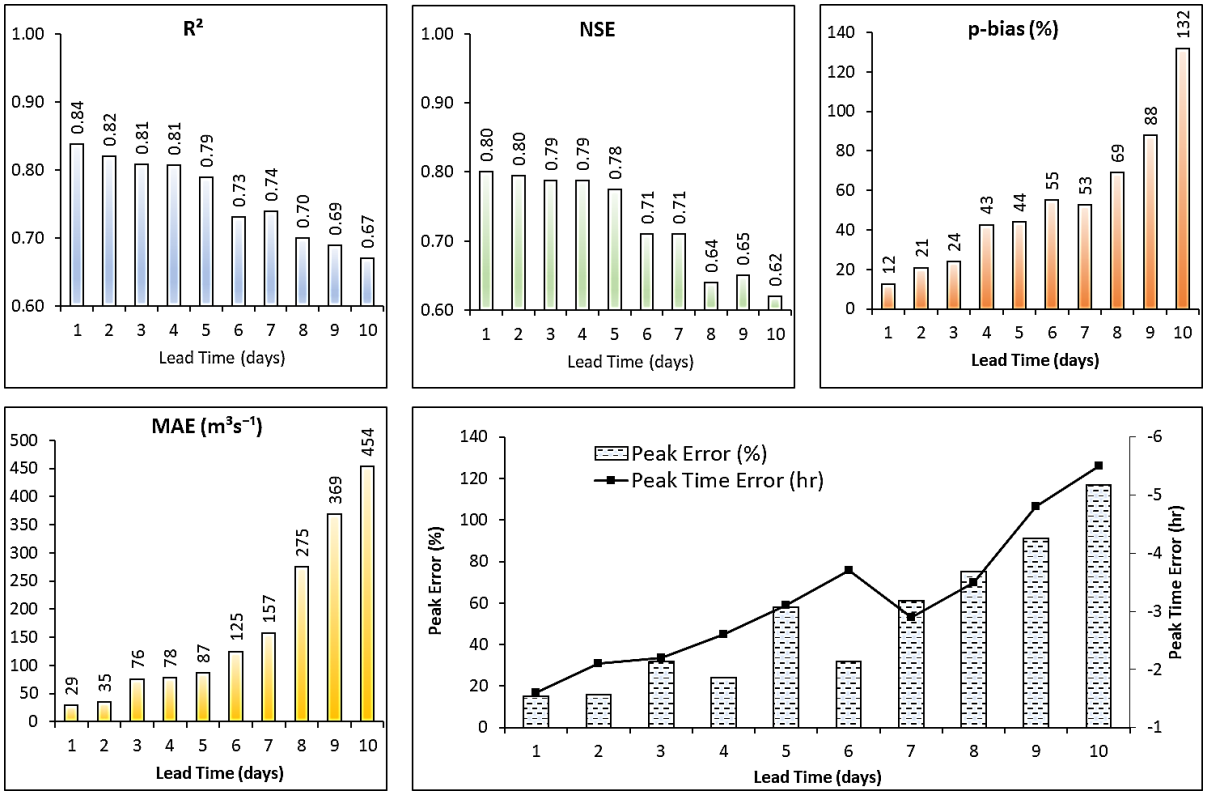

Fig. 9 Performance measures by the NAM-HD model at Sangam station for 1–10 days forecast lead-times using ECMWF data.

4.4. Updating of integrated MIKE 11 NAM-HD model using MIKE 11 FF

For testing the updating skills of the MIKE 11 FF system, the discharge values of river Jhelum at Sangam station for the flood of August 2013 were chosen. The disparities in observed and simulated values of discharges during flood simulations can be attributed to uncertainties in input meteorological data, or inefficient calibration of NAM and HD parameters. MIKE 11 FF routine allows correction of both amplitude errors and phase errors. Existing phase errors after

586 calibration were reduced to zero. Analysis period was taken as 216 hours or 9 days (hindcast
587 period). A considerably long analysis period is taken to enable detection of phase errors. The
588 value of alpha was calibrated 0.002 keeping the adjust factor as 0. For correcting the
589 discrepancies between observed and simulated values of discharge, these values were
590 compared in the hindcast period. The updated forecast results for various lead times are
591 presented in Fig. 10.

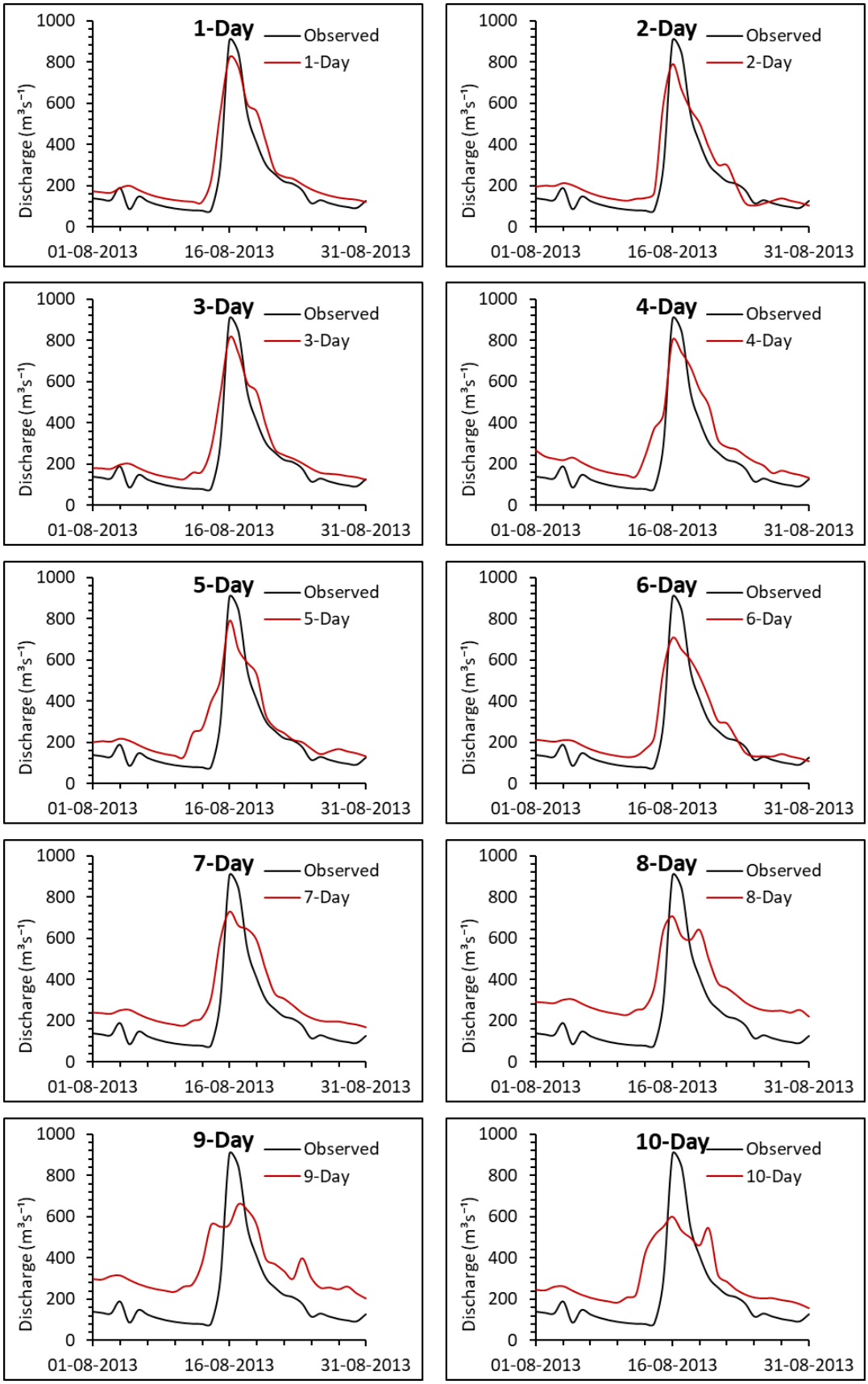

592

593 **Fig. 10 Time series plot at Sangam station for various lead times using forecasted**

594 **ECMWF data and MIKE 11 FF updating.**

The updating routine of MIKE 11 FF adequately simulated the flows predicted by using ECMWF forecasted data up to 7-days lead time. The errors in peak flow become more substantial for longer lead times. Errors in occurrence of peak flow were corrected using forecast updating. The comparative performance of the developed flood forecasting model after updating at different lead times is presented in table. Peak time error after updating was reduced to zero for 1-day, 2-day and 3-day forecast lead time while the error was below 1.0 hour for up to 7-day lead time. Deviations between observed and predicted peak flows increases with the increase in forecast lead time. The performance of the integrated NAM-HD model improved significantly after including the updating routine. Values of R^2 and NSE indicate good model performance with ECMWF input for forecast lead times up to 7 days.

Table 11 Performance of integrated NAH-HD model and FF updating model for different forecast lead-times.

Lead Time (day)	R^2	MAE	NSE	p-bias (%)	RMSE (m^3s^{-1})	Peak Error (%)	Peak Time Error (h)
1	0.9	35.9	0.9	-12.9	46.1	9.0	0.0
2	0.9	60.9	0.8	-16.3	73.6	12.4	0.0
3	0.9	61.6	0.8	-23.3	70.9	10.1	0.0
4	0.9	90.2	0.7	-36.8	95.5	11.1	0.1
5	0.8	75.3	0.7	-26.5	93.0	12.5	0.4
6	0.8	70.7	0.8	-20.5	81.8	21.6	0.7
7	0.8	113.4	0.7	-43.2	115.3	19.1	1.2
8	0.7	159.8	0.6	-63.2	159.4	21.3	2.1
9	0.6	169.7	0.5	-64.7	177.8	26.9	4.6
10	0.5	128.6	0.4	-41.1	151.8	43.3	7.8

Model updating suitably improves the efficiency of the model while reducing amplitude and phase errors. Although some errors exist in the model hydrograph even after updating, but the results are acceptable. The updated NAM-HD model with ECMWF input can thus be used for efficient flood forecasting in the Jhelum basin.

5. Conclusions

The significance of early flood forecasting for decision makers of flood risk management depends on the practical efficiency of the forecasting technique. Among various methods, computer-based deterministic hydrodynamic or rainfall-runoff models, or both, are used for flood forecasting. In this study, the MIKE 11 FF error-updating model was integrated with

MIKE 11 NAM and HD model to forecast the discharge in river Jhelum. The emphasis of this study was to present a first modelling attempt for early flood forecasting of river Jhelum using satellite-based precipitation and temperature forecasts. A hydrological model MIKE 11 NAM was coupled with a hydraulic model MIKE 11 HD to simulate discharges at four principal gauging stations of river Jhelum. Errors in flood prediction were reduced by including an automatic updating routine MIKE 11 FF in the model. The practical efficiency of the forecasting system, in a comprehensive essence, depends on the length of lead time and accuracy of forecast. Forecasted meteorological inputs contribute to increase the lead time of forecast. Integration of MIKE 11 HD model with MIKE11 NAM model removed considerable error, resulting in a high coefficient of determination (>8.0) at all the stations for both calibration and validation periods. NSE values (>0.75) suggest acceptability of model throughout the simulation period. Various error statistics were low for the integrated NAM-HD model and the results were improved by including the updating routine in the model. ECMWF ERA5 inputs were found to forecast the river discharge well in advance at 1- to 7-day lead-times. The results show that ECMWF meteorological forecasts can be used as a suitable option for real-time flood forecasting in data-scare regions. Overall, the proposed study can address the problem of early flood forecasting in Kashmir valley with sufficient lead time.

Despite the overall good performance of the model, the errors in results can be attributed to several reasons like insufficient rainfall gauging network density, large missing values in discharge, limited number of river cross sections and low-resolution topography data. Using the developed model, more accuracy in forecasting can be obtained if the following recommendations are addressed:

1. Using modern measurement system and continuous collection of real-time data.
2. Using high resolution DEMs or land surface data for accurate delineation of catchment and river networks.
3. Other satellite-based forecasted precipitation and meteorological inputs might result in improved results and enhanced forecast lead times.

The forecasting model proposed in this research can play a pivotal role in reliable early flood warnings data scarce and snowmelt-dominated Jhelum Basin. It can aid in the initiation of necessary arrangements, prompt emergency service, and evacuation before disastrous flood events. The model can also aid decision and policy makers to improve the flood control and disaster reduction policies, and accomplish a sufficient economic, social and environmental

benefits more effectively. Modelling procedure used in the study is general and can be applied for similar basins globally.

APPENDIX A

The performance of model is evaluated using various statistical performance indicators, which provide a wider assessment of the developed model. Performance indices used in this study are described in Table A.

Table A. Statistical performance indices used in this study.

S. No.	Statistical Index	Description	Equation	Value for perfect fit
1.	Correlation coefficient (r)	Goodness of fit indicator	$r = \frac{N\sum_{i=1}^{N} y_i^{obs} y_i^{pre} - \sum_{i=1}^{N} y_i^{obs} \sum_{i=1}^{N} y_i^{pre}}{\sqrt{\left[N\sum_{i=1}^{N}(y_i^{obs})^2 - \left(\sum_{i=1}^{N} y_i^{obs}\right)^2\right]\left[N\sum_{i=1}^{N}(y_i^{pre})^2 - \left(\sum_{i=1}^{N} y_i^{pre}\right)\right.}}$	1
2.	Coefficient of Determination (R^2)	Relationship between observed and predicted values.	$R^2 = \frac{\sum_{i=1}^{N}(y_i^{obs} - \bar{y}_i^{obs})(y_i^{pre} - \bar{y}_i^{pre})}{\sqrt{\sum_{i=1}^{N}(y_i^{obs} - \bar{y}_i^{obs})^2}\sqrt{\sum_{i=1}^{N}(y_i^{pre} - \bar{y}_i^{pre})^2}}$	1
3.	Mean Absolute Error (MAE)	Measure of average deviation of flow.	$MAE = \frac{1}{N}\sum_{i=1}^{N}\lvert y_i^{obs} - y_i^{pre}\rvert$	0
4.	Nash-Sutcliffe Efficiency (NSE)	Accuracy of model outputs	$NSE = 1 - \frac{\sum_{i=1}^{N}(y_i^{obs} - y_i^{pre})^2}{\sum_{i=1}^{N}(y_i^{obs} - \bar{y}_i^{obs})^2}$	1
5.	Percent **bias** (p-Bias)	Measure of over or underestimation of models.	$p-bias = \frac{\sum_{i=1}^{N}(y_i^{obs} - y_i^{pre}) \times 100}{\sum_{i=1}^{N}(y_i^{obs})}$	0
6.	Root mean Square Error (RMSE)	Measure of scatter of residuals (flow)	$RMSE = \sqrt{\frac{1}{N}\sum_{i=1}^{N}(y_i^{obs} - y_i^{pre})^2}$	0

Where,

$\mathbf{N}$ = No. of Observations

y_i^{obs} = Observed data

y_i^{pre} = Predicted data

$\bar{y}_i^{obs}$ = Mean of observed data

Acknowledgements

The authors are thankful to College of Agricultural Engineering and Technology, SKUAST-Kashmir for providing all facilities to carry out the research. The authors also acknowledge the Regional Meteorological Centre, Srinagar of India Meteorological Department, Agromet Field Unit Srinagar, and Planning and Design Division of Irrigation and Flood Control Department, Jammu and Kashmir, for providing the necessary data for the study.

Author's contributions

The authors' participations in the article are:

Conceived and designed the analysis: Sabah Parvaze

Collected the data: Sabah Parvaze and Saqib Parvaze Allaie

Contributed data or analysis tools: Junaid Nazir Khan

Performed the analysis: Sabah Parvaze, Junaid Nazir Khan, Rohitashw Kumar and Saqib Parvaze Allaie

Wrote the paper: Sabah Parvaze

Writing—review and editing: Rohitashw Kumar

Supervision: Junaid Nazir Khan

Corresponding author: Sabah Parvaze

Authors' Declarations

Funding: There are no funding sources for the research.

Conflicts of interest/Competing interests: The authors don't have any conflict of interests or any competing interests for the research.

Ethics approval: Not Applicable

Consent to participate: The authors express their consent to participate for research and review.

Consent for publication: The authors express their consent for publication of research work.

Availability of data and material: The data cannot be made available because of the policy of data providing agency.

Code availability: Not Applicable

References

Ahmad L, Habib Kanth R, Parvaze S, Sheraz Mahdi S, Ahmad L, Habib Kanth R, Parvaze S, Sheraz Mahdi S (2017) Agro-climatic and Agro-ecological Zones of India. In: Experimental Agrometeorology: A Practical Manual. Springer International Publishing, pp 99–118

Ahmad T, Pandey AC, Kumar A (2019) Evaluating urban growth and its implication on flood hazard and vulnerability in Srinagar city, Kashmir Valley, using geoinformatics. Arab J Geosci 12:1–20. https://doi.org/10.1007/s12517-019-4458-1

Ahmed F (2010) Numerical modeling of the Rideau Valley Watershed. Nat Hazards 55:63–84. https://doi.org/10.1007/s11069-010-9588-4

Alam A, Ahmad S, Bhat MS, Ahmad B (2015) Tectonic evolution of Kashmir basin in northwest Himalayas. Geomorphology 239:114–126. https://doi.org/10.1016/j.geomorph.2015.03.025

Alam A, Bhat MS, Farooq H, Ahmad B, Ahmad S, Sheikh AH (2018) Flood risk assessment of Srinagar city in Jammu and Kashmir, India. Int J Disaster Resil Built Environ 9:114–129. https://doi.org/10.1108/IJDRBE-02-2017-0012

Alfredo Mahar AMF, Racoma BA, Aracan KA, Alconis-Ayco J, Saddi IL (2017) Disseminating near-real-time hazards information and flood maps in the Philippines through Web-GIS. J Environ Sci (China) 59:13–23. https://doi.org/10.1016/j.jes.2017.03.014

Altaf F, Meraj G, Romshoo SA (2013) Morphometric Analysis to Infer Hydrological Behaviour of Lidder Watershed, Western Himalaya, India. Geogr J 2013:1–14. https://doi.org/10.1155/2013/178021

Asghar MR, Ushiyama T, Riaz M, Miyamoto M (2019) Flood and inundation forecasting in the sparsely gauged transboundary chenab river basin using satellite rain and coupling meteorological and hydrological models. J Hydrometeorol 20:2315–2330. https://doi.org/10.1175/JHM-D-18-0226.1

Bhat MS, Ahmad B, Alam A, Farooq H, Ahmad S (2019) Flood hazard assessment of the Kashmir Valley using historical hydrology. J Flood Risk Manag 12:. https://doi.org/10.1111/jfr3.12521

714 Borsch S, Simonov Y (2016) Operational Hydrologic Forecast System in Russia. In: Flood
715 Forecasting: A Global Perspective. Elsevier Inc., pp 169–181

716 Casati B, Wilson LJ, Stephenson DB, Nurmi P, Ghelli A, Pocernich M, Damrath U, Ebert EE,
717 Brown BG, Mason S (2008) Forecast verification: Current status and future directions. In:
718 Meteorological Applications. John Wiley & Sons, Ltd, pp 3–18

719 Central Water Commission (CWC), National Remote Sensing Centre (NRSC) (2014)
720 Watershed atlas of India. 1–214. https://doi.org/10.13140/RG.2.2.30331.52009

721 Creutin JD, Borga M, Gruntfest E, Lutoff C, Zoccatelli D, Ruin I (2013) A space and time
722 framework for analyzing human anticipation of flash floods. J Hydrol 482:14–24.
723 https://doi.org/10.1016/j.jhydrol.2012.11.009

724 Dar RA, Chandra R, Romshoo SA, Lone MA, Ahmad SM (2015) Isotopic and
725 micromorphological studies of Late Quaternary loess-paleosol sequences of the Karewa
726 Group: Inferences for palaeoclimate of Kashmir Valley. Quat Int 371:122–134.
727 https://doi.org/10.1016/j.quaint.2014.10.060

728 De Roo APJ, Gouweleeuw B, Thielen J, et al (2003) Development of a european flood
729 forecasting system. Int J River Basin Manag 1:49–59.
730 https://doi.org/10.1080/15715124.2003.9635192

731 DHI (2017) MIKE 11: A Modeling System for Rivers and Channels, Reference Manual,
732 Danish Hydraulic Institute, Denmark.

733 Di Baldassarre G, Castellarin A, Brath A (2009) Analyse des effets de la surélévation des levées
734 sur la propagation des crues: Exemple du Fleuve Pô, Italie. Hydrol Sci J 54:1007–1017.
735 https://doi.org/10.1623/hysj.54.6.1007

736 Dike J, Tilburg C (2007) Climatic timescale temperature and precipitation increases on Long
737 Island, New York. Atmos - Ocean 45:93–105. https://doi.org/10.3137/ao.450203

738 Doulgeris C, Georgiou P, Papadimos D, Papamichail D (2011) Evaluating three different
739 model setups in the MIKE 11 NAM model. In: Advances in the Research of Aquatic
740 Environment. Springer Berlin Heidelberg, pp 241–249

741 He Z, Hu H, Tian F, Ni G, Hu Q (2017) Correcting the TRMM rainfall product for hydrological
742 modelling in sparsely-gauged mountainous basins. Hydrol Sci J 62:306–318.
743 https://doi.org/10.1080/02626667.2016.1222532

744 Himayoun D, Mohsin F, Roshni T (2020) Efficacy in simulating the peak discharge response
745 using soft computing techniques in the Jhelum river basin, India. Int J River Basin Manag
746 18:81–93. https://doi.org/10.1080/15715124.2019.1570934

747 Jiang D, Wang K (2019) The Role of Satellite-Based Remote Sensing in Improving Simulated
748 Streamflow: A Review. Water 11:1615. https://doi.org/10.3390/w11081615

749 Jonch-Clausen T, Refsgaard JC (1984) Mathematical modelling system for flood forecasting.
750 Nord Hydrol 15:305–316. https://doi.org/10.2166/nh.1984.0027

751 Kan G, He X, Li J, Ding L, Hong Y, Zhang H, Liang K, Zhang M (2019) Computer Aided
752 Numerical Methods for Hydrological Model Calibration: An Overview and Recent
753 Development. Arch Comput Methods Eng 26:35–59. https://doi.org/10.1007/s11831-
754 017-9224-5

755 Kashani MH, Dinpashoh Y (2012) Evaluation of efficiency of different estimation methods for
756 missing climatological data. Stoch Environ Res Risk Assess 26:59–71.
757 https://doi.org/10.1007/s00477-011-0536-y

758 Khattak M, Babel M, Sharif M (2011) Hydro-meteorological trends in the upper Indus River
759 basin in Pakistan. Clim Res 46:103–119. https://doi.org/10.3354/cr00957

760 Khu ST, Liong SY, Babovic V, Madsen H, Muttil N (2001) Genetic programming and its
761 application in real-time runoff forecasting. J Am Water Resour Assoc 37:439–451.
762 https://doi.org/10.1111/j.1752-1688.2001.tb00980.x

763 Kong X, Li Z, Liu Z (2019) Flood Prediction in Ungauged Basins by Physical-Based
764 TOPKAPI Model. Adv Meteorol 2019:. https://doi.org/10.1155/2019/4795853

765 Kumar A, Gupta AK, Bhambri R, Verma A, Tiwari SK, Asthana AKL (2018) Assessment and
766 review of hydrometeorological aspects for cloudburst and flash flood events in the third
767 pole region (Indian Himalaya). Polar Sci. 18:5–20

768 Kumar R, Acharya P (2016) Flood hazard and risk assessment of 2014 floods in Kashmir
769 Valley: a space-based multisensor approach. Nat Hazards 84:437–464.
770 https://doi.org/10.1007/s11069-016-2428-4

771 Liu Z-Y, Tan B-Q, Tao X, Xie Z-H (2008) Application of a Distributed Hydrologic Model to
772 Flood Forecasting in Catchments of Different Conditions. J Hydrol Eng 13:378–384.
773 https://doi.org/10.1061/(ASCE)1084-0699(2008)13:5(378)

774 Loi NK, Liem ND, Tu LH, Hong NT, Truong CD, Tram VNQ, Nhat TT, Anh TN, Jeong J
775 (2019) Automated procedure of real-time flood forecasting in Vu Gia – Thu Bon river
776 basin, Vietnam by integrating SWAT and HEC-RAS models. J Water Clim Chang
777 10:535–545. https://doi.org/10.2166/wcc.2018.015

778 Madsen H (2000) Automatic calibration of a conceptual rainfall-runoff model using multiple
779 objectives. J Hydrol 235:276–288. https://doi.org/10.1016/S0022-1694(00)00279-1

780 Meraj G, Khan T, Romshoo SA, Farooq M, Rohitashw K, Sheikh BA (2018) An Integrated
781 Geoinformatics and Hydrological Modelling-Based Approach for Effective Flood
782 Management in the Jhelum Basin, NW Himalaya. Proceedings 7:8.
783 https://doi.org/10.3390/ecws-3-05804

784 Meraj G, Romshoo SA, Yousuf AR, Altaf S, Altaf F (2015) Assessing the influence of
785 watershed characteristics on the flood vulnerability of Jhelum basin in Kashmir Himalaya.
786 Nat Hazards 77:153–175. https://doi.org/10.1007/s11069-015-1605-1

787 Nash JE, Sutcliffe J V. (1970) River flow forecasting through conceptual models part I - A
788 discussion of principles. J Hydrol 10:282–290. https://doi.org/10.1016/0022-
789 1694(70)90255-6

790 Nielson SA, Hansen E (1973) Numerical simulation of the rainfall-runoff process on a daily
791 basis. Nord Hydrol 4:171–190. https://doi.org/10.2166/nh.1973.0013

792 Parvaze S, Khan JN, Kumar R, Allaie SP (2021) Temporal flood forecasting for trans-boundary
793 Jhelum River of Greater Himalayas. Theor Appl Climatol 2021 1–14.
794 https://doi.org/10.1007/S00704-021-03562-8

795 Paudyal GN (2002) Prévision et annonce de catastrophes hydrologiques en contexte
796 hydraulique complexe—le cas du Bangladesh. Hydrol Sci J 47:S5–S18.
797 https://doi.org/10.1080/02626660209493018

798 Rafieeinasab A, Seo DJ, Lee H, Kim S (2014) Comparative evaluation of maximum likelihood
799 ensemble filter and ensemble Kalman filter for real-time assimilation of streamflow data
800 into operational hydrologic models. J Hydrol 519:2663–2675.
801 https://doi.org/10.1016/j.jhydrol.2014.06.052

802 Rahman MM, Goel NK, Arya DS (2012) Development of the jamuneswari flood forecasting
803 system: Case study in Bangladesh. J Hydrol Eng 17:1123–1140.
804 https://doi.org/10.1061/(ASCE)HE.1943-5584.0000565

Rashid I, Romshoo SA, Chaturvedi RK, Ravindranath NH, Sukumar R, Jayaraman M, Lakshmi TV, Sharma J (2015) Projected climate change impacts on vegetation distribution over Kashmir Himalayas. Clim Change 132:601–613. https://doi.org/10.1007/s10584-015-1456-5

Refsgaard JC (1997) Validation and intercomparison of different updating procedures for real-time forecasting. Nord Hydrol 28:65–84. https://doi.org/10.2166/nh.1997.0005

Sattari MT, Rezazadeh-Joudi A, Kusiak A (2017) Assessment of different methods for estimation of missing data in precipitation studies. Hydrol Res 48:1032–1044. https://doi.org/10.2166/nh.2016.364

Schumann AH (2006) Thiessen polygon. In: Encyclopedia of Hydrology and Lakes. Springer Netherlands, pp 648–649

Schumann GJ-P, Bates PD (2018) The Need for a High-Accuracy, Open-Access Global DEM. Front Earth Sci 6:225. https://doi.org/10.3389/feart.2018.00225

Sen D (2010) Flood hazards in India and management strategies. In: Natural and Anthropogenic Disasters: Vulnerability, Preparedness and Mitigation. Springer Netherlands, pp 126–146

Sheridan P, Smith S, Brown A, Vosper S (2010) A simple height-based correction for temperature downscaling in complex terrain. Meteorol Appl 17:329–339. https://doi.org/10.1002/met.177

Singh O, Kumar M (2013) Flood events, fatalities and damages in India from 1978 to 2006. Nat Hazards 69:1815–1834. https://doi.org/10.1007/s11069-013-0781-0

Sugiura A, Fujioka S, Nabesaka S, Tsuda M, Iwami Y (2016) Development of a flood forecasting system on the upper Indus catchment using IFAS. J Flood Risk Manag 9:265–277. https://doi.org/10.1111/jfr3.12248

Tabbussum R, Dar AQ (2021) Performance evaluation of artificial intelligence paradigms—artificial neural networks, fuzzy logic, and adaptive neuro-fuzzy inference system for flood prediction. Environ Sci Pollut Res 1–18. https://doi.org/10.1007/s11356-021-12410-1

Thielen J, Bartholmes J, Ramos M-H, de Roo A (2009) The European Flood Alert System – Part 1: Concept and development. Hydrol Earth Syst Sci 13:125–140. https://doi.org/10.5194/hess-13-125-2009

836 Thompson JR, Sørenson HR, Gavin H, Refsgaard A (2004) Application of the coupled MIKE
837 SHE/MIKE 11 modelling system to a lowland wet grassland in southeast England. J
838 Hydrol 293:151–179. https://doi.org/10.1016/j.jhydrol.2004.01.017

839 Vallejo Orti M, Negussie KG (2019) Temporal statistical analysis and predictive modelling of
840 drought and flood in Rundu–Namibia. Clim Dyn 53:1247–1260.
841 https://doi.org/10.1007/s00382-019-04808-y

842 Wani MH, Baba SH, Bhat A, Chair RG (2019) Economic Appraisal of Water-Ecosystem in
843 Jammu and Kashmir: India. Int J Environ Clim Chang 9:193–203

844

Figures

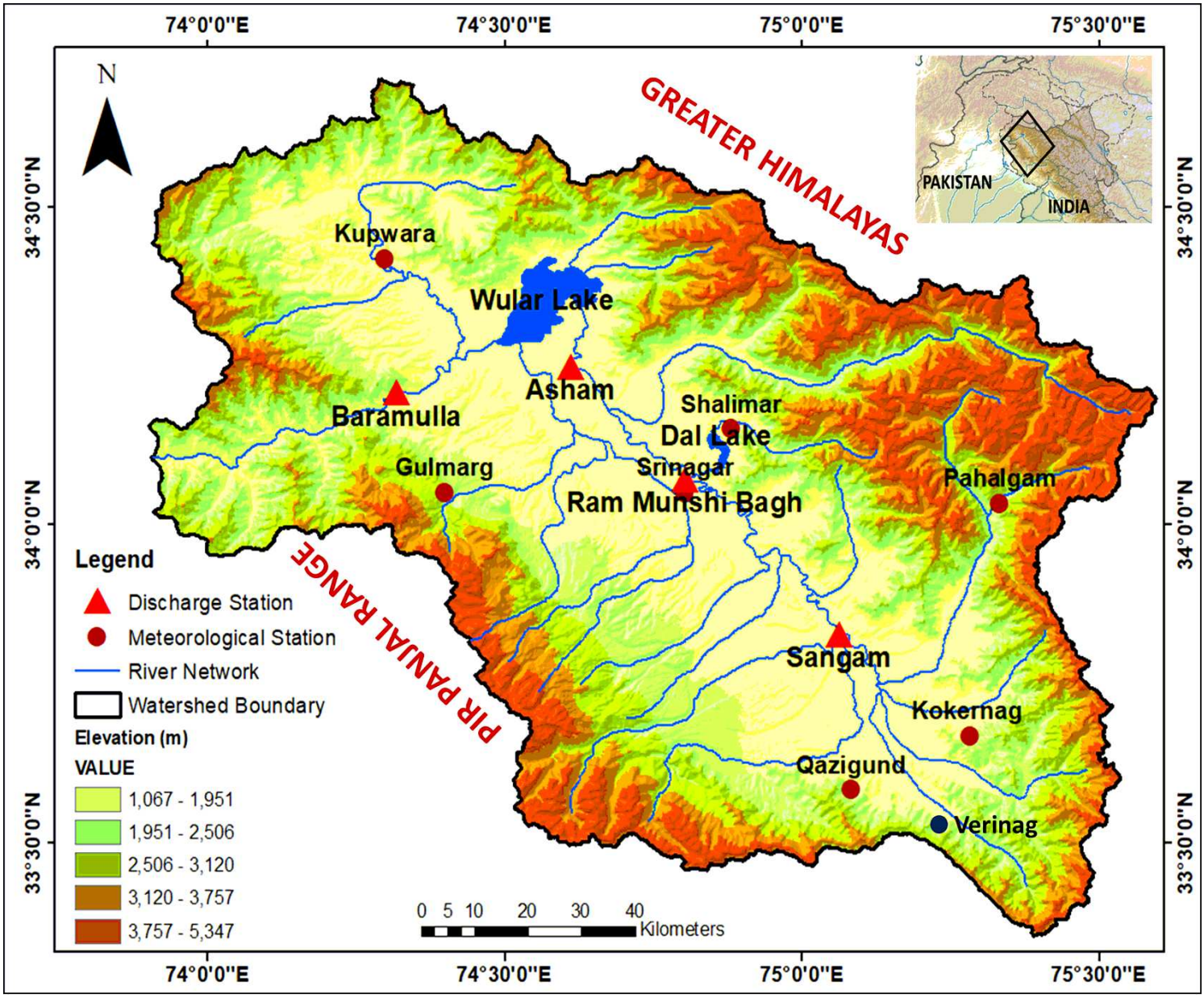

Figure 1

Location map of Kashmir valley showing the elevation zones, Jhelum river network, meteorological stations and discharge stations. Note: The designations employed and the presentation of the material on this map do not imply the expression of any opinion whatsoever on the part of Research Square concerning the legal status of any country, territory, city or area o bbnhjr of its authorities, or concerning the delimitation of its frontiers or boundaries. This map has been provided by the authors.

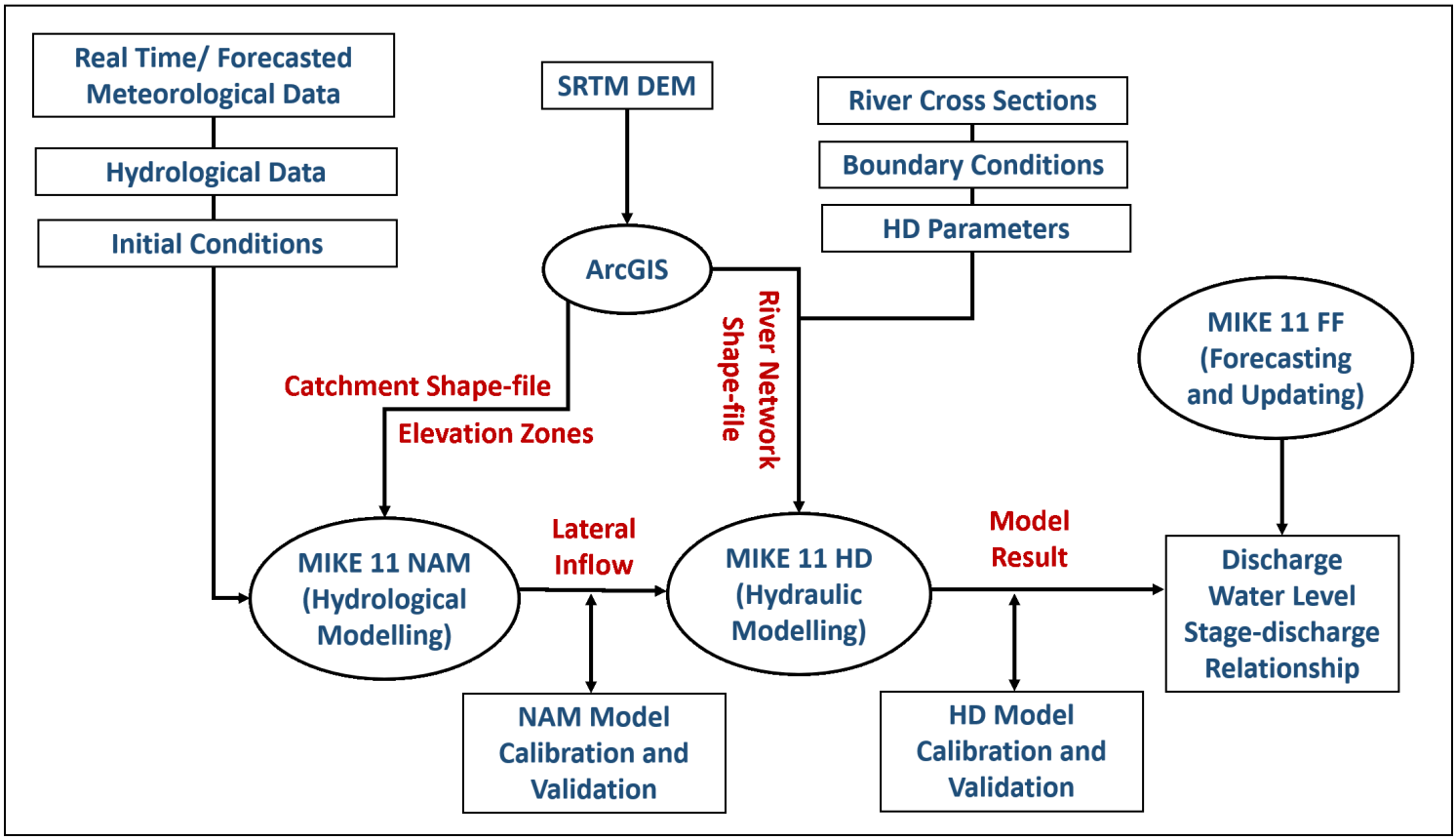

Figure 2

Flowchart for development of the flood forecasting system for Jhelum basin.

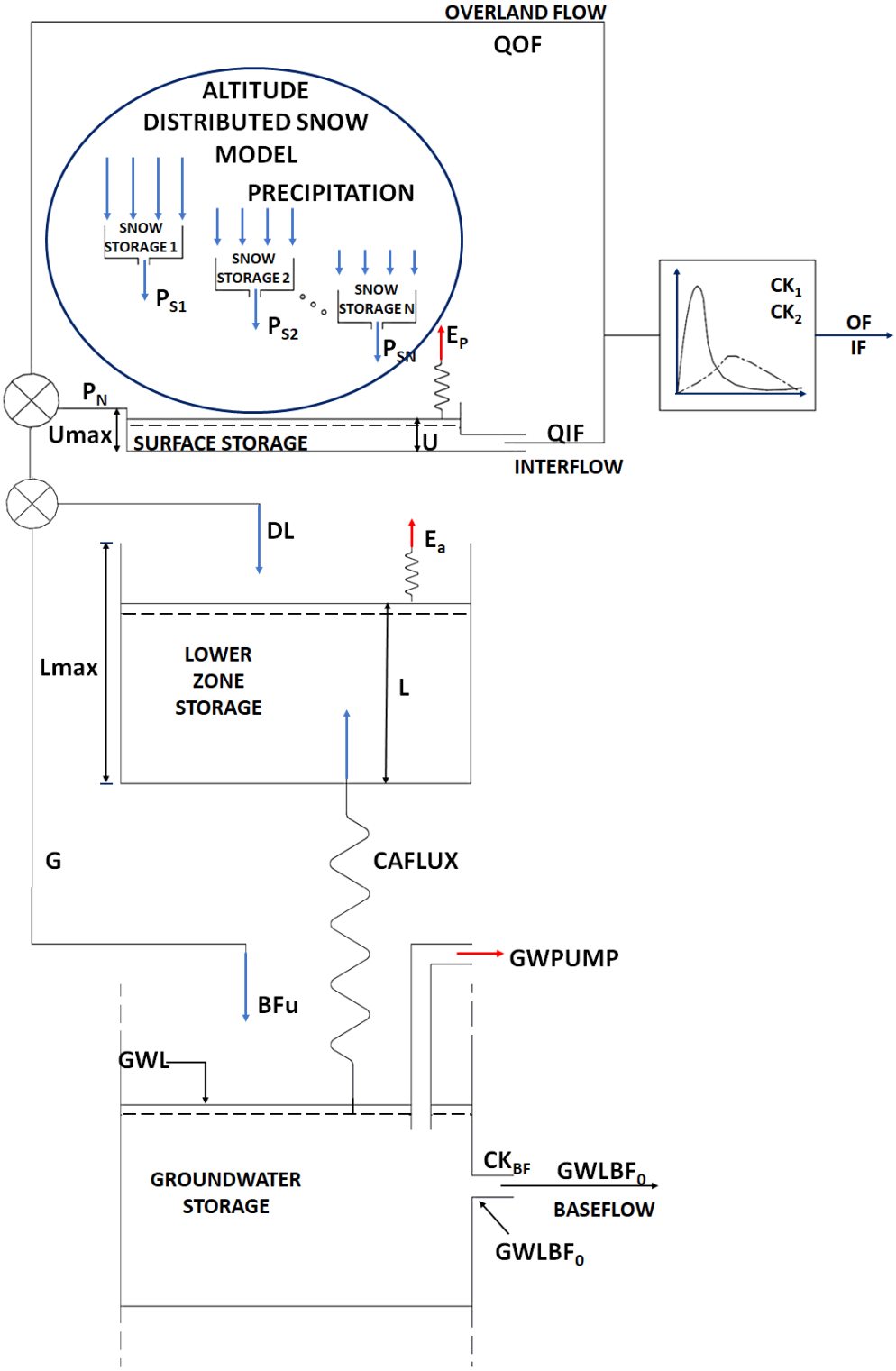

Figure 3

Structure of the NAM model showing the extended altitude distributed snow model.

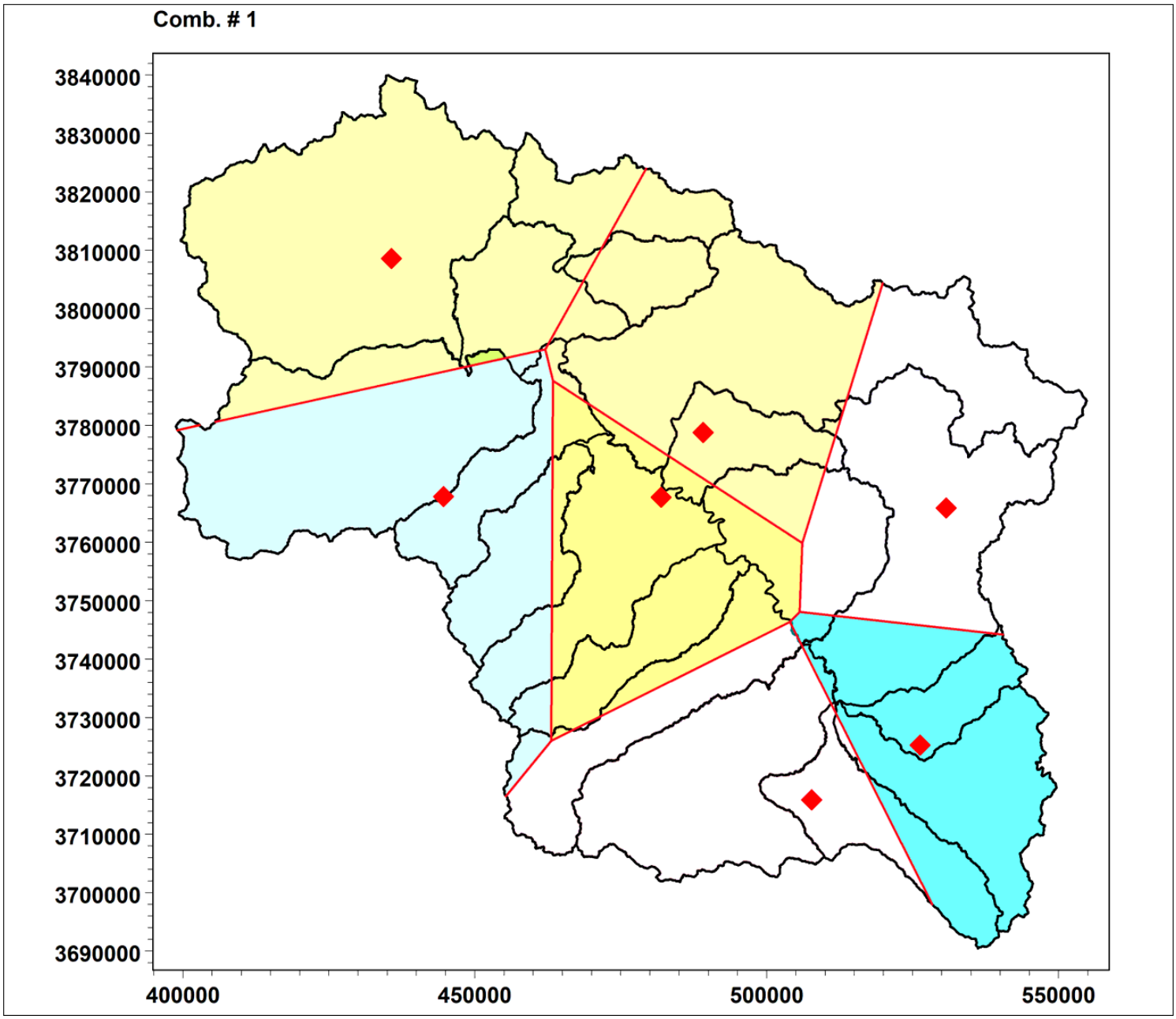

Figure 4

Sub-catchments of Jhelum basin and Thiessen polygons of different rainfall stations.

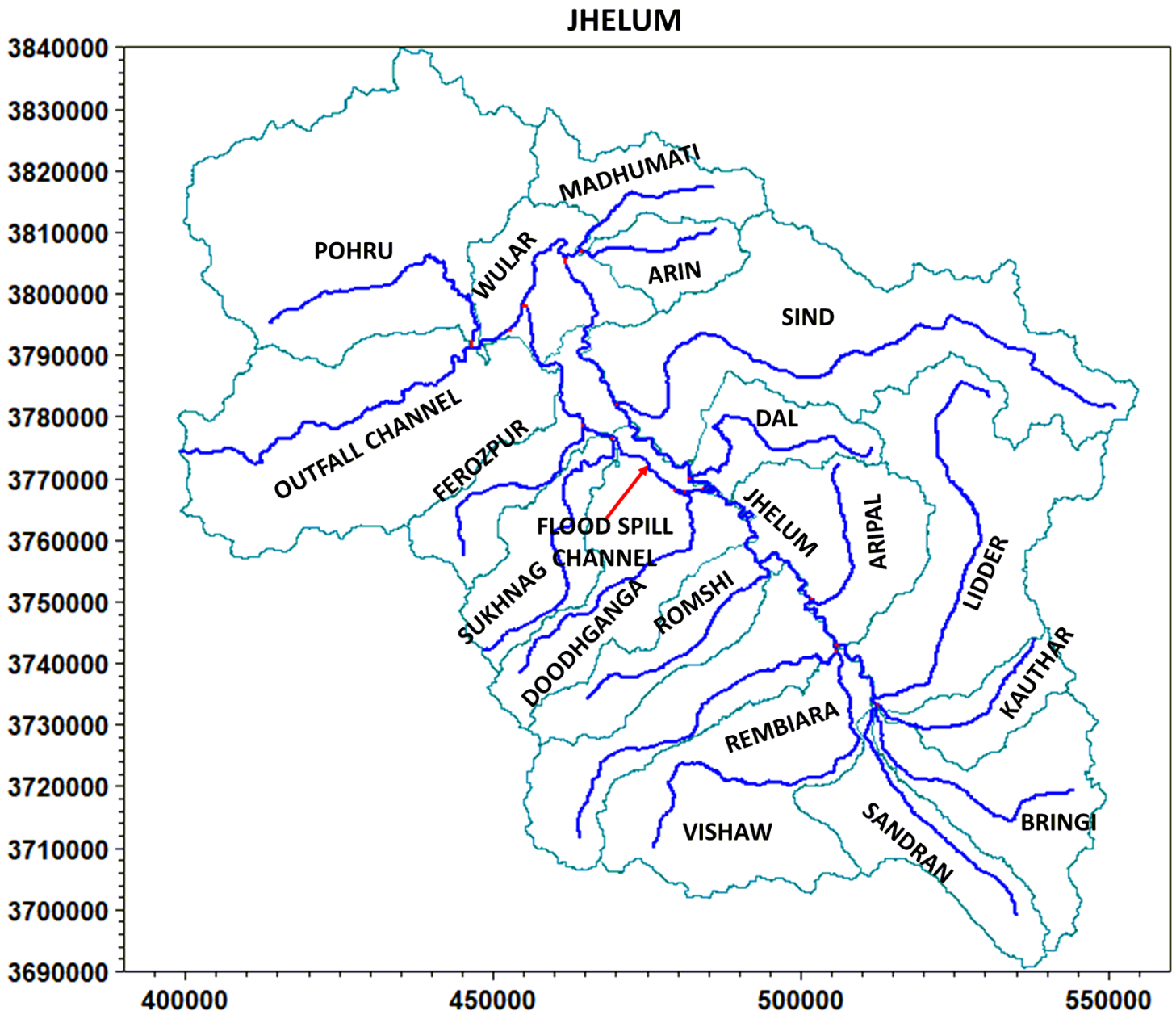

Figure 5

Jhelum river network used for setting up MIKE 11 HD model. (The axis units are UTM coordinates in meters)

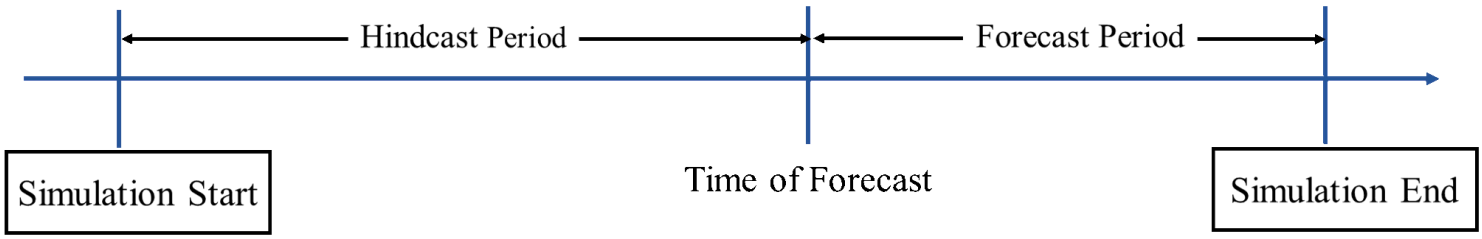

Figure 6

Conceptual flowchart of simulation period in forecasting procedure

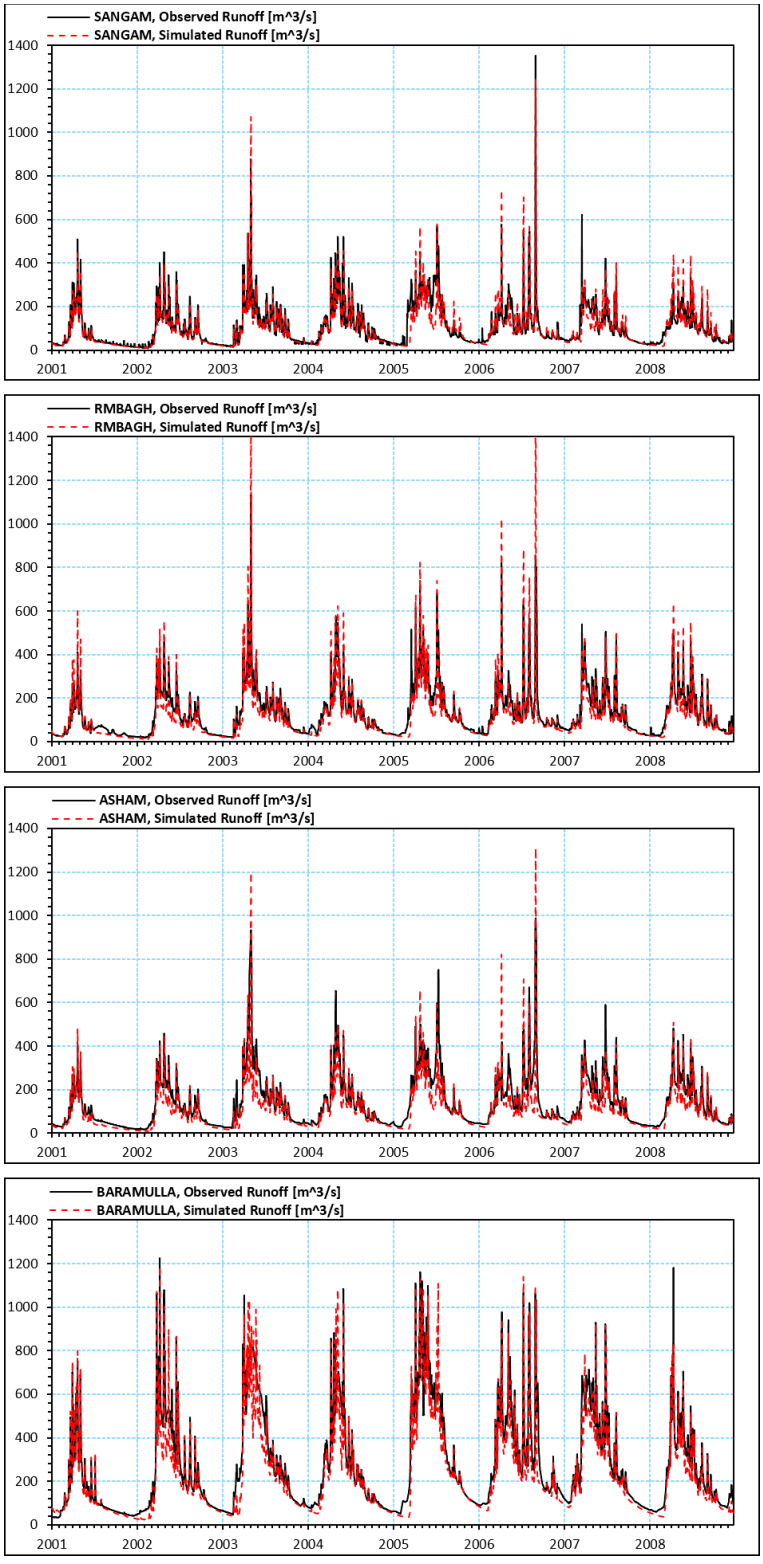

Figure 7

Time series plots of observed and simulated data at various stations for calibration period (2001-2008).

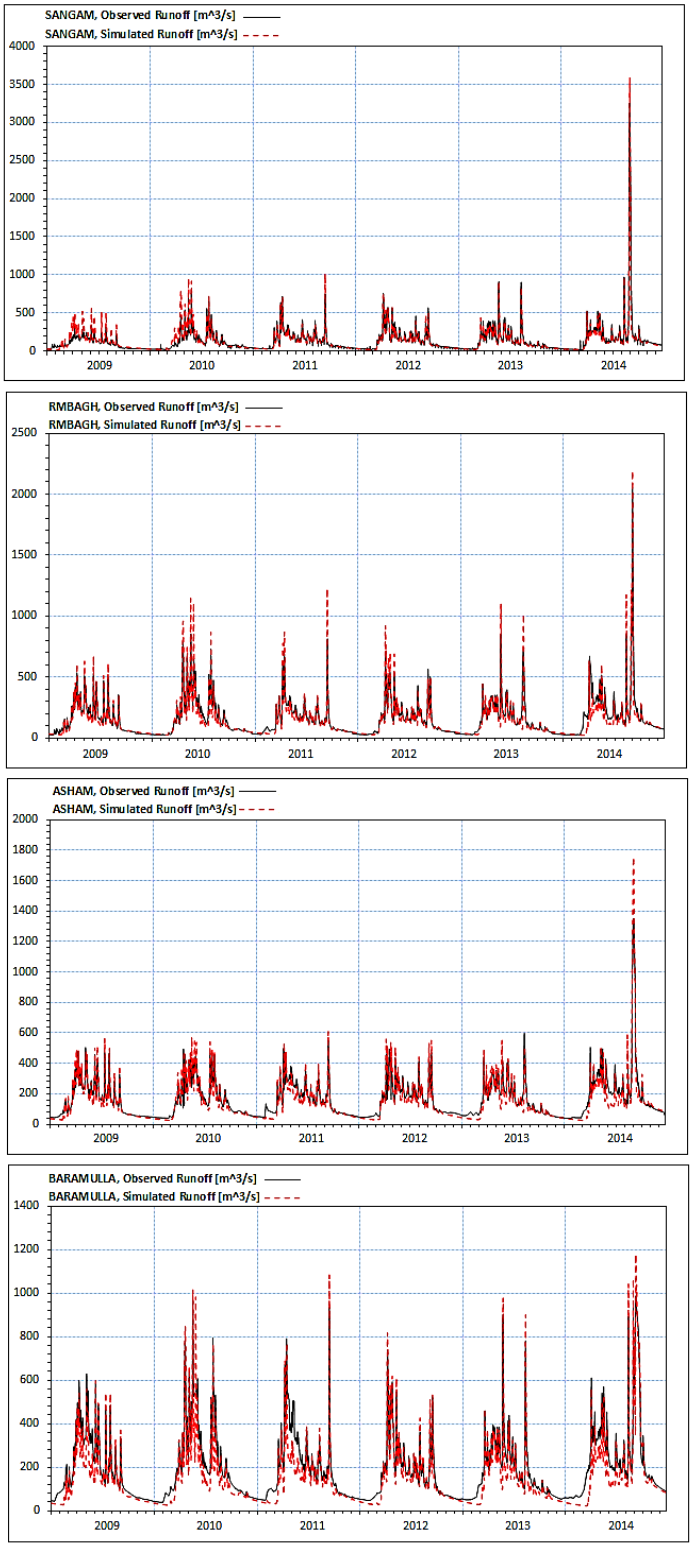

Figure 8

Time series plots of simulated versus observed discharge values at various discharge stations of river Jhelum for validation period (2009-2014).

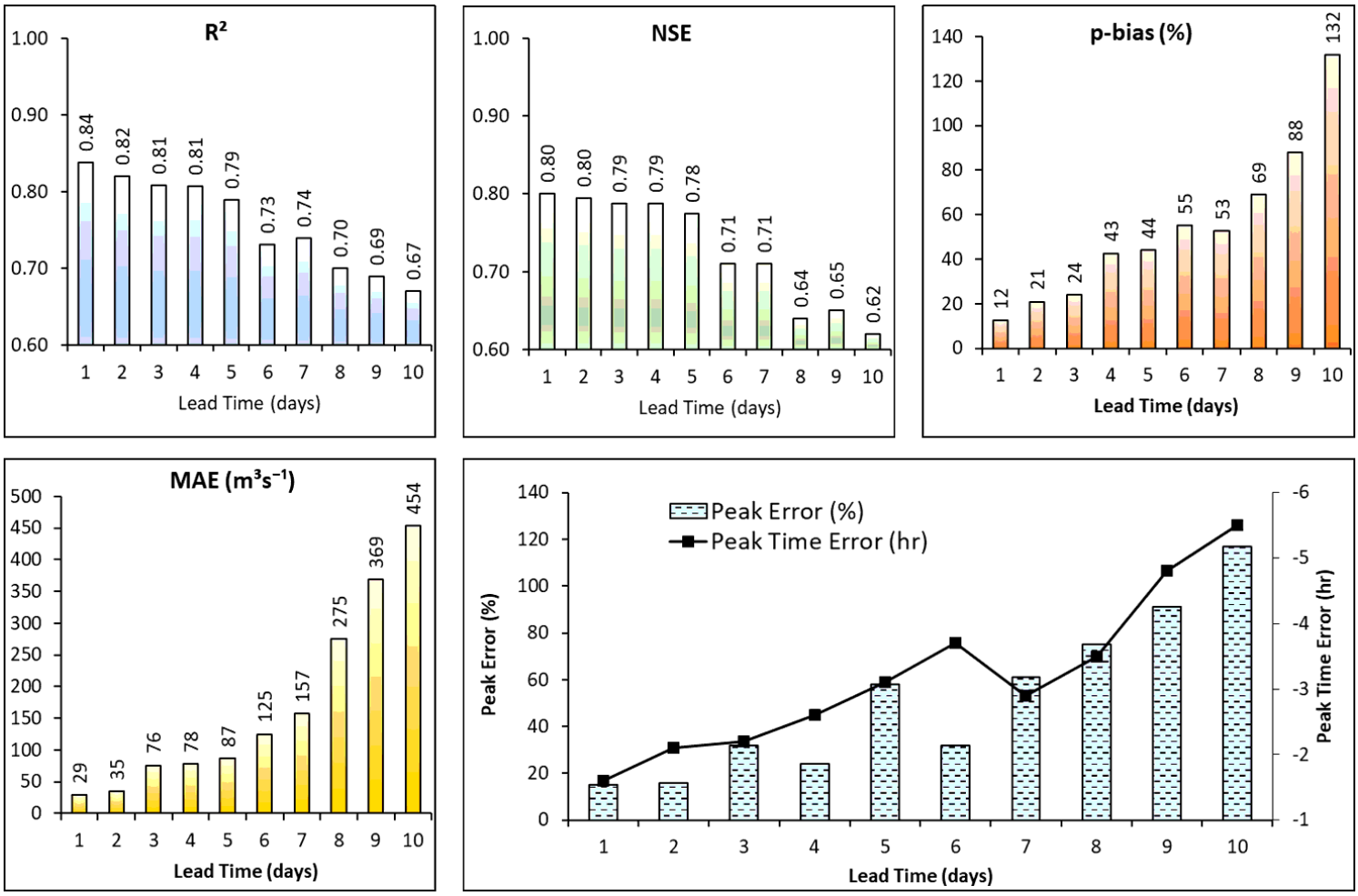

Figure 9

Performance measures by the NAM-HD model at Sangam station for 1–10 days forecast lead-times using ECMWF data.

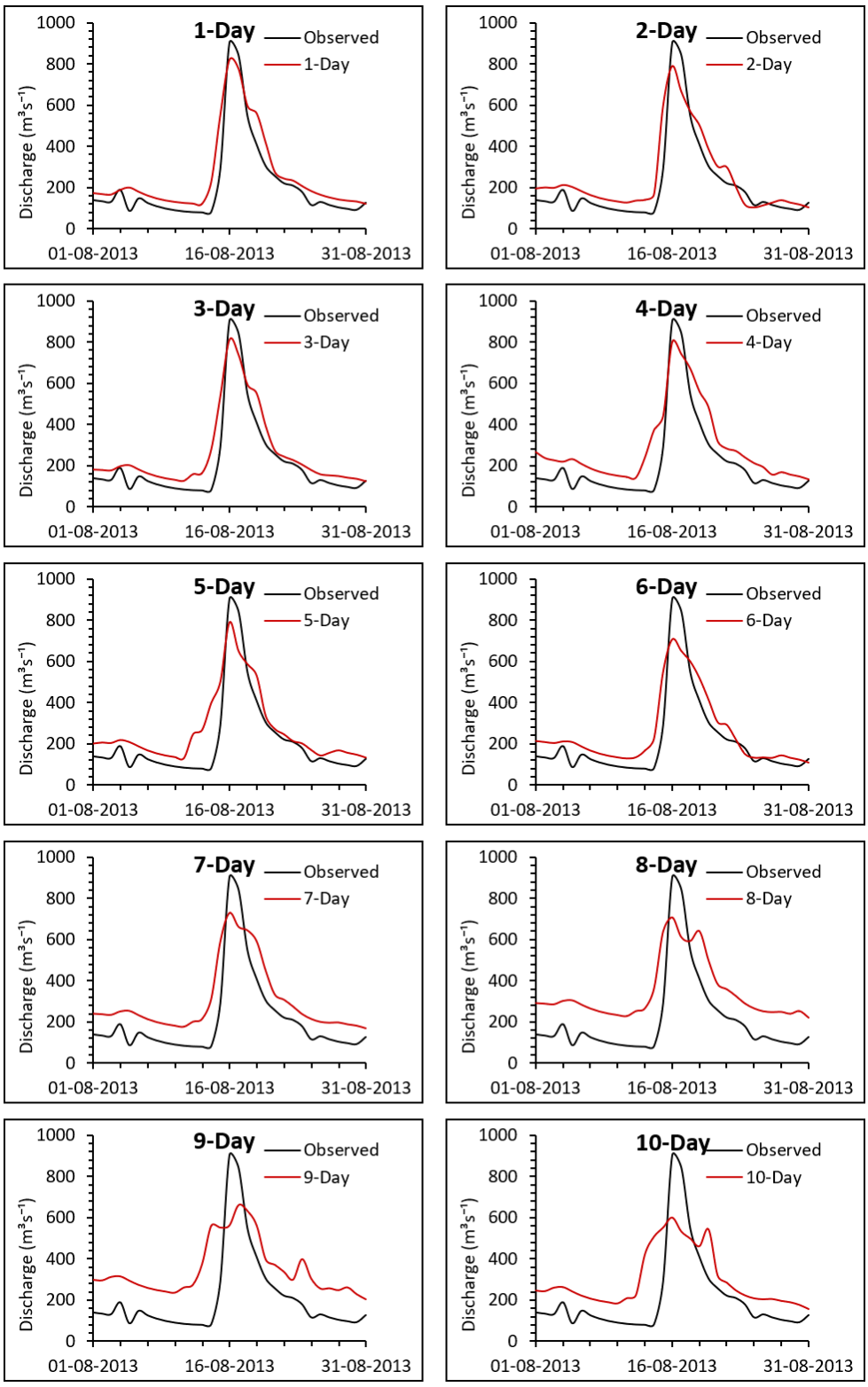

Figure 10

Time series plot at Sangam station for various lead times using forecasted ECMWF data and MIKE 11 FF updating.